Appendix B1
Water Supply Sub-Team Members

Appendix B1—Water Supply Sub-Team Members

The information presented in the Water Supply Assessment Technical Report is the outcome of a collaborative process involving representatives of numerous organizations.

A list of Water Supply Sub-Team members (as of January 31, 2011) and their affiliations is presented below.

- Carly Jerla, Bureau of Reclamation
- Armin Munévar, CH2M HILL
- Jerry Zimmerman, Colorado River Board of California
- John Whipple, New Mexico Interstate Stream Commission
- Robert Kirk, Navajo Nation
- John Gerstle, Trout Unlimited
- Chuck Cullom, Central Arizona Project
- Robert King, Utah Division of Natural Resources
- Mike Roberts, The Nature Conservancy
- Steve Cullinan, U.S Fish and Wildlife Service

Points of contact with other organizations provided additional information, as listed below.

- Subhrendu Gangopadhyay, Bureau of Reclamation's Technical Service Center
- Levi Brekke, Bureau of Reclamation's Technical Service Center
- Joe Barsugli, University of Colorado and the National Oceanic and Atmospheric Administration
- Ben Harding, AMEC Earth & Environmental

Appendix B2
Supplemental Water Supply Methods

Appendix B2—Supplemental Water Supply Methods

This appendix provides supplemental information related to the water supply methods used in the Technical Report. As discussed in the report, the analyses and discussion is centered around the water supply indicators summarized in Table B2-1. Additional detail on the methods used to assess these indicators for water supply is supplied in this appendix.

TABLE B2-1
Summary of the Water Supply Indicators for the Water Supply Assessment

Water Supply Indicator	Relevance	Temporal Scale	Spatial Scale	Method of Analysis	Method of Display
CLIMATE					
Temperature	Identification of trends in climate patterns	Monthly, Seasonal, Annual, Decadal	Grid-cell, Select Watersheds, and Basin-wide	Statistical analysis of trends and variability	Spatial analysis and visualization
Precipitation	Identification of trends in climate patterns	Monthly, Seasonal, Annual, Decadal	Grid-cell, Select Watersheds, and Basin-wide	Statistical analysis of trends and variability	Spatial analysis and visualization
HYDROLOGIC PROCESSES					
Runoff	Identification of changes in runoff processes; identification of "productive" watersheds	Monthly, Seasonal, Annual, Decadal	Grid-cell, Select Watersheds, and Basin-wide	Calculated as unit runoff; Statistics to be generated	Spatial analysis and visualization
Evapotranspiration	Identification of changes in natural losses; identification of "water stressed" watersheds	Monthly, Seasonal, Annual, Decadal	Grid-cell, Select Watersheds, and Basin-wide	Calculated as unit actual ET; Statistics to be generated	Spatial analysis and visualization
Snowpack Accumulation and Snowmelt	Identification of spatial changes in snowpack development and timing of melt	Monthly, Seasonal, Annual, Decadal	Grid-cell, Select Watersheds, and Basin-wide	Calculated as unit SWE; Peak and Timing	Spatial analysis and visualization
Soil Moisture	Identification of causes of drought and severe drying conditions; Identification of watersheds most impacted	Monthly, Seasonal, Annual, Decadal	Grid-cell, Select Watersheds, and Basin-wide	Calculated as percentage of maximum	Spatial analysis and visualization
STREAMFLOW					
Intervening and Total Natural Flows at 29 Basin Locations	Identification of changes in streamflow trends and variability	Monthly, Annual, 1-, 3-, 5-, 10-yr, and Multi-decadal	Accumulated Flow at Point	Statistical analysis of trends and variability; drought and surplus statistics	Table and box-whisker of statistics, Basin-scale maps

TABLE B2-1
Summary of the Water Supply Indicators for the Water Supply Assessment

Water Supply Indicator	Relevance	Temporal Scale	Spatial Scale	Method of Analysis	Method of Display
CLIMATE TELECONNECTIONS					
El Nino – Southern Oscillation (ENSO)	Identify changes in teleconnections and influence on regional climate; Identify relationship between long-term and shorter-term climate indices	Season, Annual, Decadal	Global/Regional	Statistical analysis of correlation between indicator and streamflow	Correlation plots and statistics
Pacific Decadal Oscillation (PDO)	Identify changes in teleconnections and influence on regional climate; Identify relationship between long-term and shorter-term climate indices	Annual, Decadal	Global/Regional	Statistical analysis of correlation between indicator and streamflow	Correlation plots and statistics
Atlantic Multidecadal Oscillation (AMO)	Identify changes in teleconnections and influence on regional climate; Identify relationship between long-term and shorter-term climate indices	Annual, Decadal	Global/Regional	Qualitative discussion	Qualitative discussion

1.0 Climate

Historical daily temperature and precipitation data were processed into monthly average temperature and monthly total precipitation for the period of 1950 to 2005 and stored in a single netCDF file to facilitate visualization and animation. The monthly, seasonal, and annual statistics were computed for each parameter and for each grid cell for the period of 1971-2000 to facilitate comparisons to projected future conditions. This 1971-2000 historical base period was selected as the most current 30-year climatological period as described by NOAA (2010) and is used as the basis for comparing to future climate projections[1].

Future climate change projections are made primarily on the basis of GCM simulations under a range of future emission scenarios. A total of 112 future climate projections used in the IPCC AR4, subsequently bias corrected and spatially downscaled (BCSD), were obtained from LLNL under the WCRP's CMIP3. This archive contains climate projections generated from 16 different GCMs developed by national climate centers and for Special Report on Emissions Scenarios (SRES) Emission Scenarios A2, A1b, and B1. These projections have been bias corrected and spatially downscaled to one-eighth-degree (~12-kilometer) resolution over the contiguous United States through methods described in detail in Wood et al. (2002), Wood et al. (2004), and Maurer (2007).

Of the six emission scenarios included in the IPCC AR4, three were selected to drive the CMIP3 multi-model dataset—A2 (high), A1B (medium), and B1 (low). The A2 Scenario is

[1] A new 30-year historical base period (1981-2010) will be issued by NOAA towards the end of 2011.

representative of high population growth, slow economic development, and slow technological change. It is characterized by a continuously increasing rate of GHG emissions, and features the highest annual emissions rates of any scenario by the end of the 21st-century. The A1B Scenario features a global population, which peaks mid-century, and rapid introduction of new and more efficient technologies balanced across both fossil- and non-fossil-intensive energy sources. As a result, GHG emissions in the A1B Scenario peak around mid-century. Lastly, the B1 Scenario describes a world with rapid changes in economic structures toward a service and information economy. GHG emission rates in this scenario peak prior to mid-century, and are generally the lowest of the scenarios. The best estimates of global temperature change during the 21st-century for each of the A2, A1B, and B1 Scenarios is 3.4°C, 2.8°C, and 1.8°C, respectively[2] (IPCC, 2007).

Bias correction is necessary to adjust a given climate projection for inconsistencies between the simulated historical climate data and observed historical climate data, which are the result of GCM bias. In the BCSD approach, projections are bias corrected using a quantile mapping technique. Following bias correction, the adjusted climate projection data are statistically consistent with the observed climate data for the historical overlap period, which is 1950 to 1999 in the Study. Beyond the historical overlap period (i.e., 2000 to 2099), the adjusted climate projection data reflect the same relative changes in mean, variance, and other statistics between the future (2000 to 2099) and historical periods (1950 to 1999) as were present in the unadjusted dataset, but the adjusted climate projection data are mapped onto the observed dataset variance. Note that this methodology assumes that the GCM biases have the same structure during the 20th and 21st-centuries simulations.

The CMIP3 multi-model dataset consists of 112 unique climate projections. Sixteen GCMs were coupled with the three emissions scenarios described previously to generate these projections. Many of the GCMs were simulated multiple times for the same emission scenario due to differences in starting climate system state or initial conditions, thus the number of available projections is greater than simply the product of GCMs and emission scenarios. Table B2-2 summarizes the GCMs, initial conditions, and emissions scenario combinations featured in the CMIP3 dataset. Initial conditions (initial atmosphere and ocean conditions used in a GCM simulation) for the 21st-century are defined by the 20th-century "control" simulation. A description of the 20th-century "control" simulations corresponding to each GCM simulation in Table B2-2 can be found at http://www-pcmdi.llnl.gov/ipcc/time_correspondence_summary.htm.

TABLE B2-2
WCRP CMIP3 Multi-Model Dataset GCMs, Initial Conditions, and Emissions Scenarios
Source: Maurer 2007

Modeling Group, Country	WCRP CMIP3 I.D.	A2	A1b	B1	Primary Reference
Bjerknes Centre for Climate Research	BCCR-BCM2.0	1	1	1	Furevik et al., 2003
Canadian Centre for Climate Modeling & Analysis	CGCM3.1 (T47)	1...5	1...5	1...5	Flato and Boer, 2001

[2] Temperature change reflects the difference between the global average in the 2090 to 2099 period relative to the global average in the 1980 to 1999 period.

TABLE B2-2
WCRP CMIP3 Multi-Model Dataset GCMs, Initial Conditions, and Emissions Scenarios
Source: Maurer 2007

Modeling Group, Country	WCRP CMIP3 I.D.	A2	A1b	B1	Primary Reference
Meteo-France/Centre National de Recherches Meteorologiques, France	CNRM-CM3	1	1	1	Salas-Melia et al., 2005
CSIRO Atmospheric Research, Australia	CSIRO-Mk3.0	1	1	1	Gordon et al., 2002
U.S. Dept. of Commerce/NOAA/Geophysical Fluid Dynamics Laboratory, USA	GFDL-CM2.0	1	1	1	Delworth et al., 2006
U.S. Dept. of Commerce/NOAA/Geophysical Fluid Dynamics Laboratory, USA	GFDL-CM2.1	1	1	1	Delworth et al., 2006
National Aeronautics and Space Administration (NASA)/Goddard Institute for Space Studies, USA	GISS-ER	1	2, 4	1	Russell et al., 2000
Institute for Numerical Mathematics, Russia	INM-CM3.0	1	1	1	Diansky and Volodin, 2002
Institut Pierre Simon Laplace, France	IPSL-CM4	1	1	1	IPSL, 2005
Center for Climate System Research (The University of Tokyo), National Institute for Environmental Studies, and Frontier Research Center for Global Change (JAMSTEC), Japan	MIROC3.2 (medres)	1...3	1...3	1...3	K-1 model developers, 2004
Meteorological Institute of the University of Bonn, Meteorological Research Institute of KMA	ECHO-G	1...3	1...3	1...3	Legutke and Voss, 1999
Max Planck Institute for Meteorology, Germany	ECHAM5/ MPI-OM	1...3	1...3	1...3	Jungclaus et al., 2006
Meteorological Research Institute, Japan	MRI-CGCM2.3.2	1...5	1...5	1...5	Yukimoto et al., 2001
National Center for Atmospheric Research, USA	CCSM3	1...4	1...3, 5...7	1...7	Collins et al., 2006
National Center for Atmospheric Research, USA	PCM	1...4	1...4	2...3	Washington et al., 2000
Hadley Centre for Climate Prediction and Research/Met Office, UK	UKMO-HadCM3	1	1	1	Gordon et al., 2000

2.0 Hydrologic Processes

Gridded climate and hydrologic process data generated by the Variable Infiltration Capacity (VIC) model are stored in ASCII flux files for each grid cell on a monthly time step. These results were converted from thousands of individual files to a specialized gridded format (netCDF) for analysis. This conversion allows for statistical and spatial analysis of the data and permits a better understanding of the primary factors, both climatological and hydrological, that

drive projected changes in streamflows relative to historical conditions. In addition to the primary VIC outputs of air temperature, precipitation, evapotranspiration (ET), runoff, and baseflow, total runoff (sum of baseflow and runoff) and runoff efficiency were computed at each grid cell and added to the netCDF files. Runoff efficiency is defined as the fraction of total runoff to the total precipitation.

The complete list of parameters included in the netCDF files is as follows:

- Average air temperature (°C)
- Precipitation (millimeters)
- ET (millimeters)
- Runoff (surface) (millimeters)
- Baseflow (subsurface) (millimeters)
- Total Runoff (millimeters)
- Total Runoff Efficiency (percent)
- Soil Moisture (millimeters)
- Maximum Soil Moisture (millimeters)
- Soil Moisture Fraction (percent)
- SWE (millimeters)

One netCDF file was produced for each climate projection and for the historical scenario, for a total of 113 netCDF files. As with the climate data, monthly, seasonal, and annual statistics were derived for the hydrologic process information for the historical period 1971-2000 and three future 30-year climatological periods: 2011-2040, 2041-2070, and 2066-2095. The historical period of 1971 to 2000 is selected as the reference climate since it is the currently established climate normal used by NOAA and represents the most recent time period. Representative statistics described previously were generated on a monthly, seasonal, and annual basis. In this analysis, the seasons are defined as follows: Fall: October, November, December (OND), Winter: January, February, March (JFM); Spring: April, May, June (AMJ); and Summer: July, August, September (JAS).

The statistical analysis was conducted on both a grid cell and watershed basis. The results of the grid cell analysis produce the most informative map graphics and clearly show spatial variation at the greatest resolution possible. At this spatial scale, the statistics for each grid cell are developed independently. The resulting statistics are stored in netCDF files. Monthly time series data were extracted from these files to characterize patterns of change in hydrologic parameters.

Finally, "change metrics" are generated for each parameter in which the difference between future period statistics and historical period statistics are calculated on both absolute and percent change bases. These results are again stored in netCDF files, with two files generated for each future period—one for grid cell data and one for watershed data. The format of these files is identical to those containing the results of the statistical analysis.

3.0 Climate Teleconnections

During the past 30 years, the understanding of the climatic importance of the oceans, particularly ocean temperature, has steadily improved (U.S. Department of Interior, 2004). Initial research focused on the distant effects of the recurrent warming of the equatorial Pacific Ocean referred to as El Niño, which South American fishermen have long known to have an adverse effect on the

coastal fisheries in Peru. El Niño is the warm phase of the sea-surface temperature component of a coupled ocean-atmosphere process called ENSO, which spans the equatorial Pacific Ocean. The atmospheric component, the Southern Oscillation, refers to a "seesaw" effect in sea-level pressure between the tropical Pacific and Indian Oceans. Reduced sea-level pressure in the Pacific combined with increased sea-level pressure in the Indian Ocean leads to a weakening in the trade winds over the eastern Pacific. This weakening enables warm water from the central equatorial Pacific to spread eastward and southward along the west coast of South America, creating the classic El Niño condition. Conversely, and about as frequently, the sea-level pressure in the Pacific Ocean increases while pressure in the Indian Ocean decreases, which causes trade winds to intensify over the eastern Pacific. When this occurs, equatorial upwelling of deep, cold water and cold water from the west coast of South America are pulled northward and westward from the coast into the eastern and central Pacific, producing La Niña. Thus, El Niño and La Niña are, respectively, the warm and cold phases of the coupled ENSO system.

ENSO events typically last from 6 to 18 months and, therefore, are the single most-important factor affecting inter-annual climatic variability on a global scale (Diaz and Kiladis, 1992). ENSO has been linked to the occurrence of flooding in the lower Colorado River Basin (Webb and Betancourt, 1992) and to both floods and droughts across the western United States (Cayan et al., 1999). Warm winter storms have been enhanced during El Niño, causing above-average runoff and floods in the Southwest, such as during 1982 to 1983. However, not all El Niño events lead to increased runoff in the Southwest. For example, during the 2002 to 2003 warm episode, runoff was below average in the Colorado River Basin. Similarly, La Niña is frequently, though not always, associated with below-average flow in the Colorado River. As a result, although ENSO exerts a strong influence in modulating wet versus dry conditions in many parts of the United States, the effect is not always the same in any given region. Some condition other than ENSO must also be influencing weather and climate patterns affecting the Colorado River.

In the mid-1990s, scientists identified another ocean temperature pattern, this one occurring in the extratropical Pacific Ocean north of 20ºN (Mantua and Hare, 2002), which was named the PDO. The PDO varies or oscillates on a decadal scale of 30 to 50 years for the total cycle; that is, much of the North Pacific Ocean will be predominantly though not uniformly warm (or cool) for periods of about 15 to 25 years. During the 20th-century, the PDO exhibited several phases−warmer along coastal southeastern Alaska from 1923 to 1943 and again from 1976 to 1998, and cooler from 1944 to 1975. Since 1999, the PDO has exhibited higher-frequency fluctuations, varying from cool (1999 to 2001) to warm (2002 to 2004). Currently, the causes of the variations in the PDO are unknown and its potential predictability is uncertain. Recent research indicates that the PDO phase may be associated with decadal-length periods of above- and below-average precipitation and streamflow in the Colorado River basin (Hidalgo, 2004) but, as with ENSO, such associations are not always consistent.

Climate teleconnections were first analyzed by selecting indices that could have potential influence in streamflow changes for the Colorado River Basin. As previously mentioned, published research indicates that the strongest correlations with Colorado River Basin flows were observed with the PDO and ENSO indices. For ENSO, data were collected for both the ocean component (sea surface temperature anomolies) and the atmospheric component. The two components are highly correlated and combined describe ENSO. The Southern Oscillation Index (SOI), the atmospheric component, was the primary dataset utilized in the Study due to the longer availability of information. Therefore, the quantitative teleconnections analysis was based

on the PDO index and the SOI. Only a qualitative discussion of the AMO is included in the Technical Report.

Annual averages of the PDO on water year basis were calculated and compared with the same water year annual flows. Annual average values for the SOI were computed, using different annual windows. The average SOI index presented in the Study refers to the June to November period, a period that was identified as a strong indicator of ENSO events (Redmond and Koch, 1991). Once the SOI averages were computed, ENSO events were determined by years when the averaged SOI was below -1 (classified as an El Niño year) or above 1 (classified as a La Niña year). A warm PDO was defined as a PDO value greater than or equal to 0.0 and a cold PDO was a PDO value less than 0.0. AMO research by Mo et al. (2009) indicates that the direct influence of the AMO on drought is small. The major influence of the AMO is to modulate the impact of ENSO on drought. The influence is large when the sea surface temperature anomalies (SSTAs) in the tropical Pacific and in the North Atlantic are opposite in phase. A cold (warm) event in a positive (negative) AMO phase amplifies the impact of the cold (warm) ENSO on drought. The ENSO influence on drought is much weaker when the SSTAs in the tropical Pacific and in the North Atlantic are in phase. With a cycle of approximately 70 years, AMO research is constrained by the observed data record of approximately 150 years. AMO research continues in this area using indirect observations of tree rings and sedimentary layers.

4.0 Streamflow

Two historical streamflow data sets, the observed record spanning the period 1906-2007 and the paleo-reconstructed record spanning the period 762-2005, were utilized in the Study to characterize historical streamflow patterns and variability. Period comparisons are made between the full extent of the data and a more-recent period. For the observed dataset spanning 1906 to 2007, the second comparison period (1978-2007) was selected as the most recent 30-year period since it captures the current drought period and the apparent climate shift after 1977. For the Paleo dataset spanning 762 to 2005, the second comparison period was selected as the 1906 to 2005 such that direct comparisons could be made of the observed and paleo timeframes. Annual flows and moving averages for 3, 5, 10, 20, and 30 years were computed for the two time periods so that differences in mean flows and variability of flows could be accessed. Annual flows and moving averages were also used to evaluate minimum and maximum streamflows. Exceedance probability plots were used to evaluate the likelihood of annual flows to exceed a specified streamflow value.

Under the Downscaled GCM Projected scenario, the routed streamflow from the VIC simulations was utilized to characterize natural flows at each of the 29 flow locations. VIC-simulated runoff from each grid cell is routed to the outlet of each watershed (the 29 flow locations) using VIC's offline routing tool. The routing tool processes individual cell runoff and baseflow terms and routes the flow based on flow direction and flow accumulation inputs derived from digital elevation models. Flows are output in both daily and monthly time steps. Only the monthly flows were used in the analysis for the Study. It is important to note that VIC routed flows are considered "natural flows" in that they do not include effects of diversions, imports, storage, or other human management of the water resource. Bias-correction will be applied to the VIC-simulated flows to account for any systematic bias in the hydrology model or data sets. The evaluation of the most appropriate bias-correction scheme to implement given offsetting biases between the VIC validation period and the overlapping climate projection

period is ongoing. The flows presented in this Interim Report are considered "raw" in that no streamflow bias-correction is included.

Annual streamflows for both the historical analysis and future water supply scenarios were analyzed to provide an estimate of the inter-annual variability, or deficit and surplus conditions. Definitions of "drought" are often subjective in water planning. In general, droughts are defined as periods of prolonged dryness. The interannual variability of the climate and hydrology of the Southwest imply basins may be in frequent states of drought. As part of the analysis conducted for this report, different averaging periods for determining and measuring deficits were considered. The definition used in the remainder of this report is the following: "a deficit occurs whenever the 2-year average flow falls below the long-term mean annual flow of 1906-2007". The use of a 1-year averaging period was discarded because it implied that any one year above the 15 maf Lees Ferry natural flow would break a multi-year deficit. The use of a 2-year averaging period implies that it may take two consecutive above normal years (or one extreme wet year) to end a drought. For a basin with sizable reservoir storage in comparison to its mean flow such as the Colorado River, it may take several years to end a deficit. Averaging periods of 1- to 10-years were evaluated, following research by Timilsena et al (2007). The 2-year averaging period appeared to produce similar deficits as the longer-averaging periods.

Appendix B3
Water Supply Data Sources

Appendix B3—Water Supply Data Sources

Table B3-1 presents the data sources used in the Water Supply Assessment followed by a brief discussion of each source.

TABLE B3-1
Sources of Data Used for the Water Supply Assessment

Parameter	Description	Data Source
CLIMATE INDICATORS		
Historical Temperature and Precipitation	Historical gridded temperature and precipitation at 1/8th degree resolution for the period of 1950 to 1999. Extension through 2005 is not documented.	Maurer et al. 2002 (http://www.engr.scu.edu/~emaurer/data.shtml)
Future Temperature and Precipitation Projections	112 future monthly temperature and precipitation projections based on IPCC AR4 emission scenarios and subsequently bias-corrected and statistically downscaled to 1/8th degree resolution	Maurer et al., 2007. (http://gdo-dcp.ucllnl.org/downscaled_cmip3_projections/)
HYDROLOGIC PROCESS INDICATORS		
Evapotranspiration, Runoff, Snow Water Equivalent, Soil Moisture	VIC-simulated hydrologic fluxes and grid-cell storage terms driven by observed climatology (1950-2005) and 112 future climate projections (1950-2099)	AECOM 2010
Snowpack	Point snow water equivalent from late 1970s to present from the SNOTEL network	NRCS 2010 (http://www.wcc.nrcs.usda.gov/snow/)
TELECONNECTION INDICATORS		
El Nino Southern Oscillation	Monthly SOI for Jan 1866 through March 2010	UCAR 2010; University of East Anglia Climatic Research Unit 2010
Pacific Decadal Oscillation	Monthly PDO indices for Jan 1900 through Jan 2010	Joint Institute for the Study of the Atmosphere and Ocean (JISAO) 2010
STREAMFLOW INDICATORS		
Observed Streamflow used in the Observed Resampled Scenario	Natural streamflow for the period of 1906-2007 for the 29 streamflow locations commonly used for Reclamation planning.	Prairie and Callejo, 2005; Reclamation, 2010
Paleo Reconstructed Streamflow used in the Paleo Resampled Scenario	Reconstructed natural streamflows for the period 762-2005 at 29 locations derived from ecologically contrasting tree-ring sites in the southern Colorado Plateau during the past 2 millennia.	Reclamation 2010; Meko et al. 2007
Paleo Conditioned Streamflow used in the Paleo Conditioned Scenario	Blended paleo streamflow states with observed streamflow magnitudes at 29 locations	Prairie et al.2008

TABLE B3-1
Sources of Data Used for the Water Supply Assessment

Parameter	Description	Data Source
Future Streamflow Projections used in the Downscaled GCM Projected Scenario	VIC-simulated runoff and routed streamflow at 29 locations driven by 112 future climate projections for the period 1950-2099	AMEC 2010; Reclamation 2010

1.0 Climate

Gridded observed climate data for the period from 1950 to 1999, as developed by Maurer et al. (2002), were downloaded via the Internet from Santa Clara University (http://www.engr.scu.edu/~emaurer/ data.shtml). The data are stored in network common data form (netCDF) at one-eighth-degree resolution and contain daily temperature (min and max), precipitation, and wind speed values for the contiguous United States. Subsequent to Maurer et al. (2002), the gridded dataset was extended to 2005 using identical methods. The temperature and precipitation data were processed into monthly average temperature and monthly total precipitation to facilitate comparisons.

A total of 112 future climate projections used in the Intergovernmental Panel on Climate Change (IPCC) Fourth Assessment Report (AR4), subsequently bias-corrected and statistically downscaled (BCSD), were obtained from Lawrence Livermore National Laboratory (LLNL) under the World Climate Research Program's (WCRP) Coupled Model Intercomparison Project Phase 3 (CMIP3) (Maurer et al., 2007). This data contains monthly temperature and precipitation at the one-eighth-degree resolution. This data is available via the Web site, *Bias Corrected and Downscaled WCRP CMIP3 Climate Projections* (*http://gdo-dcp.ucllnl.org/downscaled_cmip3_projections/*), which is jointly hosted by the Green Data Oasis, Santa Clara University, Reclamation, and LLNL.

2.0 Hydrologic Parameters

The primary sources for hydrologic process data are derived from the VIC-simulated conditions driven by either observed climatology (1950-2005) or projected climate (1950-2099). VIC simulates all major moisture fluxes at the grid-cell using physically-based methods. These moisture fluxes are not generally measured at the spatial resolution necessary for basin assessments, thus the VIC-derived patterns are considered the most suitable source. Both the climate and hydrologic data are stored in ASCII formatted text files known as "flux files." One flux file is produced for every grid cell of the study area, and each file contains values for the specified parameters at every time step of the simulation.

In addition to streamflow, the VIC model exports climate and hydrologic parameter data for each simulation. These parameters are presented in the following Table B3-2:

TABLE B3-2
Climate and Hydrologic Parameters

VIC Parameter	Units
Average air temperature	degrees Celsius (°C)
Precipitation	millimeters (mm)
Evapotranspiration	mm
Runoff (surface)	mm
Baseflow (subsurface)	mm
Total runoff	mm
Soil moisture (in each of 3 soil layers)	mm
Soil moisture fraction	percent
SWE	Mm

Gridded climate and hydrologic parameter data generated by the VIC model for the historical period were stored in a specialized format (netCDF). The VIC grid cell flux data was converted to the netCDF, allowing for statistical analysis and visualization via spatial mapping. This analysis was performed to better understand the primary factors, both climatological and hydrological, that drive projected changes in streamflows relative to historic conditions.

Point snow water equivalent, precipitation, and temperature are available from the National Resources Conservation Service (NRCS) Snow-Telemetry (SNOTEL) network. Network deployment started in the late 1970s and now numbers approximately 800 stations in the 11 western states and Alaska. The data are available from Snow Survey and Water Supply Forecast Program Web sites: http://www.wcc.nrcs.usda.gov/snow/. The spatial representativeness of the SNOTEL data is uncertain (Daly et al., 2000). In preliminary results, Molotch et al. (2001) showed that SWE can begin to vary significantly beyond 500 meters from a SNOTEL site, due to terrain impacts on snow ablation, as well as small scale depositional variations. A variety of methods have been used to distribute point measurements to spatial grids. The methods used are complex and beyond the scope of the Study; therefore, site specific SNOTEL data were not processed to independently validate the SWE, precipitation, and temperature fields derived from the VIC model.

3.0 Climate Teleconnections

The teleconnections selected for the Study were the ENSO, PDO and AMO. An extensive literature review (Redmond and Koch, 1991; Diaz and Kiladis, 1992; McCabe et al. 2004, etc.) indicated that the ENSO and PDO would have the strongest correlation with Colorado River Basin streamflows; therefore, a quantitative analysis was done only for these two indices and a qualitative analysis for the AMO. ENSO and PDO datasets from appropriate federal and university sources were downloaded for the Study.

4.0 Streamflow

Observed Natural Streamflows used in the Observed Resampled Scenario: Obtained for the period of 1906 to 2007 at the 29 flow locations commonly used by Reclamation for planning.

Reclamation uses data collected from the United States Geological Survey (USGS) and other gage sites, consumptive use records, records of reservoir releases and other data to compute monthly natural flows at 29 locations throughout the Basin: 20 locations upstream of and including the Lees Ferry gaging station in Arizona, and nine locations below the Lees Ferry gaging station (Prairie and Callejo, 2005).

Natural flow for the Upper Basin is computed as follows:

Natural Flow = Historic Flow + Consumptive Uses & Losses+/- Reservoir Regulation

Historical streamflow data were obtained from USGS web pages. Total depletions in the form of consumptive uses and losses include the following: irrigated agriculture, reservoir evaporation, stockponds, livestock, thermal power, minerals, municipal and industrial (M&I) and exports/imports. Reservoir regulation includes mainstem reservoirs and non-mainstem reservoirs.

Natural flows for the Lower Basin are comprised of computed gains and losses (on the mainstem) and historical flows (on the tributaries). Computed gains and losses consider the following consumptive uses and losses: Decree Accounting data, evaporation (from Lake Mead, Mohave, and Havasu), and phreatophytes. Reservoir regulation includes change in reservoir storage and change in bank storage. Historical flows on the tributaries (i.e., Paria, Virgin, Little Colorado and Bill Williams Rivers) have not had the historical depletions added back to the gaged flow due to the state of current methods and processes. Thus, most Lower Basin flows should not be considered natural. See *Technical Report C – Water Demand Assessment Appendix C5* for more detail on the treatment of the Lower Basin tributaries.

Monthly intervening and total natural flow for the 29 locations are available. "Intervening" flows represent the flow generated between two locations, but do not include the cumulative contribution of the locations upstream. "Total" flows, on the other hand, included the local intervening flow and all upstream flows from that location.

Additional information, documentation, and the natural flow data are available at http://www.usbr.gov/lc/region/g4000/NaturalFlow/Index.html

Paleo Reconstructed Streamflow used in the Paleo Resampled Scenario: Obtained at 29 locations for the period 762 to 2005 based on streamflow reconstructions at Lees Ferry from tree-ring chronologies. The reconstructed streamflows at Lees Ferry were derived from ecologically contrasting tree-ring sites in the southern Colorado Plateau during the past 2 millennia (Meko et al. 2007). Streamflow values were disaggregated, spatially and temporally to the 29 locations by Reclamation (Prairie 2006, Prairie et al. 2006).

Paleo Conditioned Streamflow used in the Paleo Conditioned Scenario: Blends the observed historical record and Paleo-reconstructed record to generate future inflow scenarios that are comprised of magnitudes of the historical record and state information from the Paleo record provided by Reclamation (Prairie 2006, Prairie et al. 2008).

Future Streamflow Projections used in the Downscaled GCM Projected Scenario: VIC hydrologic model traces of future streamflows for the period 1950 to 2099 from 112 GCM realizations for the 29 streamflow locations within the basin. VIC model results were provided by Reclamation from contract work performed by AMEC Earth & Environmental (2010). This effort is more fully described in the Future Supply section of this Technical Report.

Appendix B4
VIC Modeling Methods

Appendix B4—VIC Modeling Methods

The VIC model (Liang et al., 1994; Liang et al., 1996; Nijssen et al., 1997) is a spatially distributed hydrologic model that solves the water balance at each model grid cell. It incorporates spatially distributed parameters describing topography, soils, land use, and vegetation classes. VIC is considered a macro-scale hydrologic model in that it is designed for larger basins with fairly coarse grids. In this manner, it accepts input meteorological data directly from global or national gridded databases or from GCM projections. To compensate for the coarseness of the discretization, VIC is unique in its incorporation of subgrid variability to describe variations in the land parameters as well as precipitation distribution. Parameterization within VIC is performed primarily through adjustments to parameters describing the rates of infiltration and baseflow as a function of soil properties, as well as the soil layers' depths. When simulating in water balance mode, VIC is driven by daily inputs of precipitation, maximum and minimum temperature, and windspeed. The model internally calculates additional meteorological forcings such as short- and long-wave radiation, relative humidity, vapor pressure, and vapor pressure deficits. Rainfall, snow, infiltration, evapotranspiration (ET), runoff, soil moisture, and baseflow are computed over each grid cell on a daily basis for the entire period of simulation. An offline routing tool then processes the individual cell runoff and baseflow terms and routes the flow to develop streamflow at various locations in the watershed. Figure B4-1 shows the hydrologic processes included in the VIC model.

FIGURE B4-1
Hydrologic Processes Included in the VIC Model
Source: University of Washington 2010

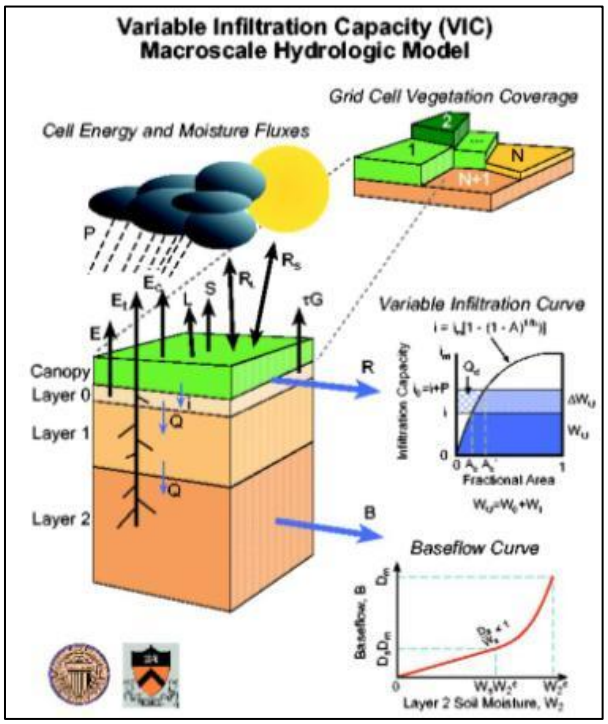

The VIC model has been applied to many major basins in the United States, including large-scale applications to California's Central Valley (Maurer et al., 2002; Brekke et al., 2007; Cayan et al., 2009), Colorado River Basin (Christensen and Lettenmaier, 2009), Columbia River Basin (Hamlet et al., 2010), and for several basins in Texas (Maurer et al., 2003; CH2M HILL, 2008). The VIC model has a number of favorable attributes for the Study, but VIC's three most significant advantages are that it has a reliable, physically based model of ET, it has a physically based model of snow dynamics, and it has been used for two studies of climate change in the Colorado River Basin for which calibrated parameters are available.

1.0 VIC Modeling Methods Specific to the Colorado River Basin

The University of Washington (Christensen and Lettenmaier, 2009) provided a preliminary calibrated VIC model of the Colorado River Basin to AMEC (2009), a consultant to Reclamation, to provide modeled VIC streamflow results. AMEC reported that the calibrated model provided excellent fit of simulated and observed streamflows for gage locations covering large basin areas (e.g., the Colorado River at the Lees Ferry gage). No re-calibration was performed as part of the Study.

1.1 Model Inputs

The VIC model was driven by meteorological forcing data. While the model has some flexibility in what variables are required, forcing files typically include daily values for precipitation, maximum temperature, minimum temperature, and windspeed. The VIC model required that the forcing files be in either American Standard Code for Information Interchange (ASCII) or binary format, with one file for each grid cell of the simulation domain. The model grid for the Basin consists of approximately 4,500 grid cells at a one-eighth-degree latitude by longitude spatial resolution.

Daily gridded observed meteorology was obtained from Santa Clara University (Maurer et al., 2002) for the period of 1950 to 1999. Projections of monthly future climate data were developed through methods described in the previous section. These BCSD projections and the process of quantile mapping create a modified daily time series that spans the same time period as the observed meteorology. Daily precipitation and temperature are adjusted based on the derived monthly changes and scaled according to the daily patterns in the observed meteorology. Wind speed was not adjusted in these analyses as downscaling of this parameter was not available, nor well-translated from global climate models to local scales.

1.2 VIC Model Processes and Output

As described previously, the VIC model was simulated in water balance mode. In this mode, a complete land surface water balance is computed for each grid cell on a daily basis for the entire model domain. Unique to the VIC model is its characterization of sub-grid variability. Sub-grid elevation bands enable more-detailed characterization of snow-related processes. Five elevation bands are included for each grid cell. In addition, VIC also includes a sub-daily (1-hour) computation to resolve transients in the snow model. The soil column is represented by three soil zones extending down from the land surface to capture the vertical distribution of soil moisture. The VIC model represents multiple vegetation types using NASA's Land Data Assimilation System (LDAS) databases as the primary input data set.

For each grid cell, the VIC model computes the water balance over each grid cell on a daily basis for the entire period of simulation. For the simulations performed for the Basin, the following water balance parameters were produced as output on a daily and monthly time-step: precipitation, runoff, baseflow, ET, soil moisture, and SWE.

The runoff simulated from each grid cell is routed to various river flow locations using VIC's offline routing tool. The routing tool processes individual cell runoff and baseflow terms and routes the flow based on flow direction and flow accumulation inputs derived from digital elevation models. For the simulations performed for the Basin, intervening streamflow was routed to 29 locations that align with the 29 natural flow locations in the Colorado River Simulation System (CRSS), Reclamation's long-term planning model and the primary modeling tool that will be used in the Study. Flows are output in both daily and monthly time steps. Only the monthly flows were used in subsequent analyses. It is important to note that VIC routed flows are considered "naturalized" in that they do not include effects of diversions, imports, storage, or other human management of the water resource.

1.3 Colorado River Basin VIC Model Validation

To ensure the VIC model was adequately calibrated, a validation simulation was performed. The validation compared the calibrated VIC model (forced with historical gridded precipitation, maximum and minimum temperature, and windspeed [documented in Maurer et al.2002, 2007]) hydrologic process outputs against observed 1950-2005 streamflow, April 1 SWE, and ET. Annual and monthly time series and scatter plots comparisons, and error and bias analysis (RMSE), for each of the 30 watersheds were completed for the validation analysis.

1.4 VIC Model Limitations

While the model contains several sub-grid mechanisms, the coarse-grid scale should be noted when considering results and analysis of local scale phenomenon. The VIC model is currently best applied for the regional scale hydrologic analyses. The model is only as good as its inputs. There are several limitations to long-term gridded meteorology related to data, spatial-temporal interpolation and bias correction that should be considered. In addition, the inputs to the model do not include any transient trends in the vegetation or water management that may affect streamflows; they should only be analyzed from a "naturalized" flow change standpoint. Finally, the VIC model includes three soil zones to capture the vertical movement of soil moisture, but does not include groundwater.

Appendix B5
Application of VIC Modeling for the Downscaled GCM Projected Scenario

Appendix B5—Application of VIC Modeling for the Downscaled GCM Projected Scenario

1.0 Future Climate and Hydrologic Modeling Methods

In many traditional analyses of water resources, the assumption that hydroclimatic trends and variability can be represented by what has occurred historically has been made. However, recent observations and future projections indicate that the climate is changing, thus magnifying the need to understand the direct linkages between climate and watershed processes. Hydrologic models, especially those with strong, direct linkages to climate such as VIC, enable these processes to be effectively characterized, and provide estimates of changes in magnitude and timing of Basin runoff with changes in climate conditions.

The data and methods applied in developing a future climate dataset, assuming potential climate change conditions, are presented followed by an overview of the hydrologic model. Lastly, the methods employed to analyze the hydrologic model outputs are discussed.

2.0 Future Climate Data Development

The production of future streamflow data via hydrologic modeling requires projected temperature and precipitation data representative of future climate conditions. When these data are derived from Global Climate Models, a nonstationary future climate can be explored. A total of 112 future climate projections used in the Intergovernmental Panel on Climate Change (IPCC) Fourth Assessment Report (AR4), subsequently Bias Corrected and Spatially Downsealed (BCSD), were obtained from Lawrence Livermore National Laboratory (LLNL) under the World Climate Research Programme's (WCRP's) Coupled Model Intercomparison Project phase 3 (CMIP3). This archive contains climate projections generated from 16 different GCMs developed by national climate centers and for Special Report on Emissions Scenarios (SRES) Emission Scenarios A2, A1B, and B1. These projections have been bias-corrected and spatially-downscaled to one-eighth-degree (~12-kilometer) resolution over the contiguous United States through methods described in detail in Wood et al. (2002), Wood et al. (2004), and Maurer (2007).

Future climate change projections are made primarily on the basis of GCM simulations under a range of future emission scenarios. Currently, there are approximately 20 major GCMs that are supported by national institutions worldwide. While GCMs have improved significantly in recent years, the models continue to have substantial uncertainty, especially for regional conditions. The coarse-scale of global models requires results be "downscaled," to apply to a region or watershed. Whether through dynamic or statistical methods, downscaling adds another source of uncertainty to projections. In addition, the range of projections, especially beyond 2030, is governed by assumed future global emissions and assumed physical processes, parameters or statistical relationships embedded in global climate models.

3.0 Emissions Scenarios

In 2000, IPCC published a special report on greenhouse gas (GHG) emissions scenarios (SRES) that described a family of six emission scenarios to condition global climate models (IPCC, 2000; 2007). The emissions scenarios are defined by alternative future development pathways, covering a wide range of demographic, economic and technological driving forces and resulting GHG emissions. The GHG emissions associated with each scenario are shown in Figure B5-1.

FIGURE B5-1
Scenarios for GHG Emissions from 2000 to 2100 in the Absence of Additional Climate Policies
Units on y-axis are billon tons of total annual emissions in equivalent carbon dioxide units
Source: IPCC 2007

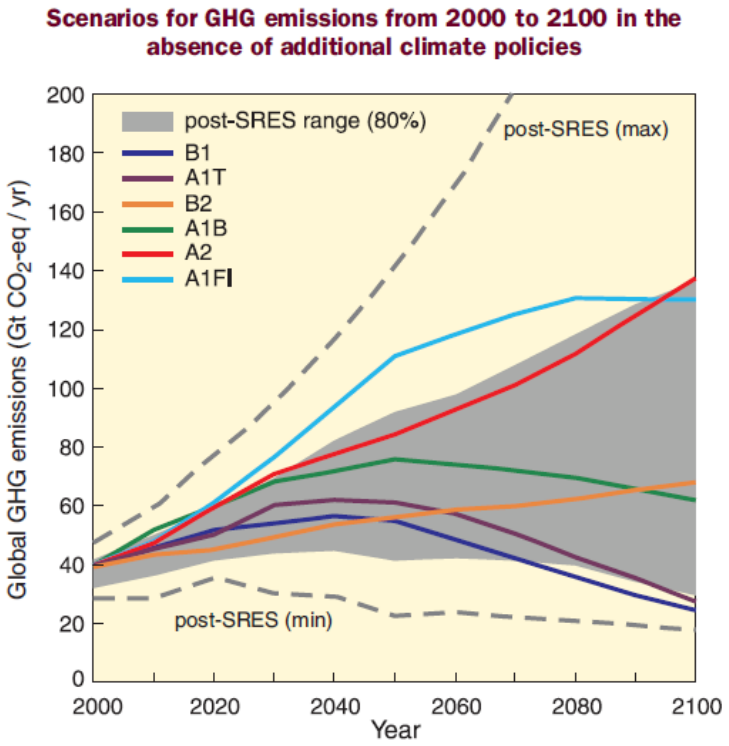

Figure 3.1. Global GHG emissions (in $GtCO_2$-eq per year) in the absence of additional climate policies: six illustrative SRES marker scenarios (coloured lines) and 80th percentile range of recent scenarios published since SRES (post-SRES) (gray shaded area). Dashed lines show the full range of post-SRES scenarios. The emissions include CO_2, CH_4, N_2O and F-gases. {WGIII 1.3, 3.2, Figure SPM.4}

Of these six scenarios, three were selected to drive the CMIP3 multi-model dataset—A2 (high), A1B (medium), and B1 (low). The A2 Scenario is representative of high population growth, slow economic development, and slow technological change. It is characterized by a continuously increasing rate of GHG emissions, and features the highest annual emissions rates of any scenario by the end of the 21st-century. The A1B Scenario features a global population, which peaks mid-century, and rapid introduction of new and more efficient technologies balanced across both fossil- and non-fossil-intensive energy sources. As a result, GHG emissions

in the A1B Scenario peak around mid-century. Lastly, the B1 Scenario describes a world with rapid changes in economic structures toward a service and information economy. GHG emission rates in this scenario peak prior to mid-century, and are generally the lowest of the scenarios. As shown in Figure B5-2, the best estimates of global temperature change during the 21st-century for each of the A2, A1B, and B1 Scenarios is 3.4°C, 2.8°C, and 1.8°C, respectively[3] (IPCC, 2007).

FIGURE B5-2
Projections of Surface Temperatures for the Selected GHG Emissions Scenarios from 2000 to 2100
Source: IPCC 2007

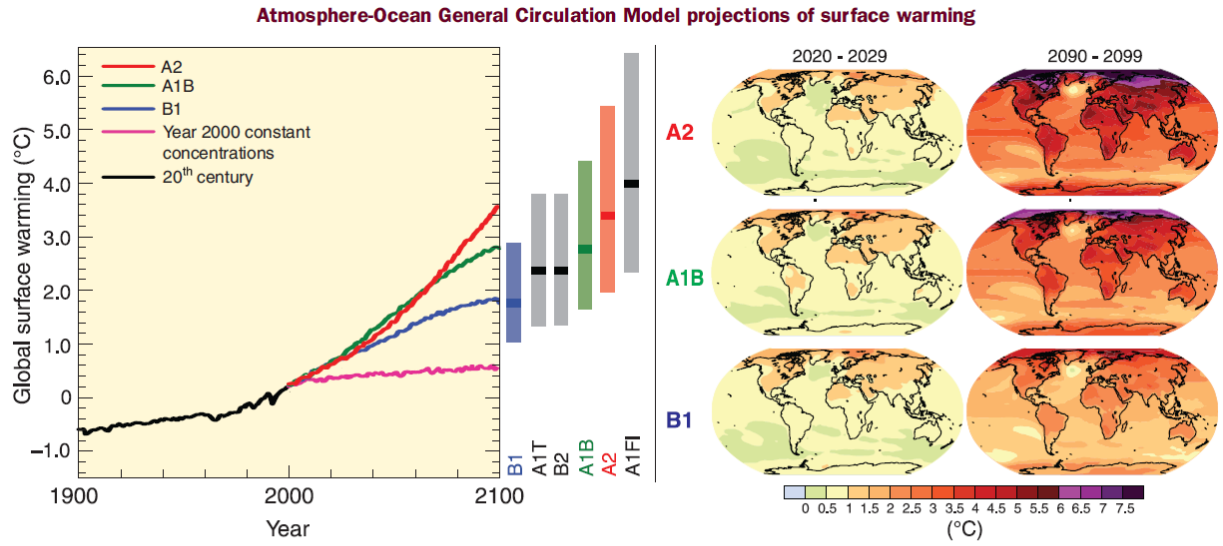

Figure 3.2. ***Left panel:*** *Solid lines are multi-model global averages of surface warming (relative to 1980-1999) for the SRES scenarios A2, A1B and B1, shown as continuations of the 20th century simulations. The orange line is for the experiment where concentrations were held constant at year 2000 values. The bars in the middle of the figure indicate the best estimate (solid line within each bar) and the likely range assessed for the six SRES marker scenarios at 2090-2099 relative to 1980-1999. The assessment of the best estimate and likely ranges in the bars includes the Atmosphere-Ocean General Circulation Models (AOGCMs) in the left part of the figure, as well as results from a hierarchy of independent models and observational constraints.* ***Right panels:*** *Projected surface temperature changes for the early and late 21st century relative to the period 1980-1999. The panels show the multi-AOGCM average projections for the A2 (top), A1B (middle) and B1 (bottom) SRES scenarios averaged over decades 2020-2029 (left) and 2090-2099 (right). {WGI 10.4, 10.8, Figures 10.28, 10.29, SPM}*

3.1 Global Climate Models (GCMs)

The CMIP3 multi-model dataset consists of 112 unique climate projections. Sixteen GCMs were coupled with the three emissions scenarios described previously to generate these projections. Many of the GCMs were simulated multiple times for the same emission scenario due to differences in starting climate system state or initial conditions, thus the number of available projections is greater than simply the product of GCMs and emission scenarios. Table B5-1 summarizes the GCMs, initial conditions (specified by the run numbers in the A2, A1B, and B1 columns), and emissions scenario combinations (A2, A1B, B1) featured in the CMIP3 dataset. Initial conditions (initial atmosphere and ocean conditions used in a GCM simulation) for the 21st-century are defined by the 20th-century "control" simulation. A description of the

[3] Temperature change reflects the difference between the global average in the 2090 to 2099 period relative to the global average in the 1980 to 1999 period.

20th-century "control" simulations corresponding to each GCM simulation in Table B2-2 can be found at http://www-pcmdi.llnl.gov/ipcc/time_correspondence_summary.htm

TABLE B5-1
WCRP CMIP3 Multi-Model Dataset GCMs, Initial Conditions, and Emissions Scenarios
Source: Maurer 2007

Modeling Group, Country	WCRP CMIP3 I.D.	A2	A1b	B1	Primary Reference
Bjerknes Centre for Climate Research	BCCR-BCM2.0	1	1	1	Furevik et al., 2003
Canadian Centre for Climate Modeling & Analysis	CGCM3.1 (T47)	1...5	1...5	1...5	Flato and Boer, 2001
Meteo-France/Centre National de Recherches Meteorologiques, France	CNRM-CM3	1	1	1	Salas-Melia et al., 2005
CSIRO Atmospheric Research, Australia	CSIRO-Mk3.0	1	1	1	Gordon et al., 2002
U.S. Dept. of Commerce/NOAA/Geophysical Fluid Dynamics Laboratory, USA	GFDL-CM2.0	1	1	1	Delworth et al., 2006
U.S. Dept. of Commerce/NOAA/Geophysical Fluid Dynamics Laboratory, USA	GFDL-CM2.1	1	1	1	Delworth et al., 2006
National Aeronautics and Space Administration (NASA)/Goddard Institute for Space Studies, USA	GISS-ER	1	2, 4	1	Russell et al., 2000
Institute for Numerical Mathematics, Russia	INM-CM3.0	1	1	1	Diansky and Volodin, 2002
Institut Pierre Simon Laplace, France	IPSL-CM4	1	1	1	IPSL, 2005
Center for Climate System Research (The University of Tokyo), National Institute for Environmental Studies, and Frontier Research Center for Global Change (JAMSTEC), Japan	MIROC3.2 (medres)	1...3	1...3	1...3	K-1 model developers, 2004
Meteorological Institute of the University of Bonn, Meteorological Research Institute of KMA	ECHO-G	1...3	1...3	1...3	Legutke and Voss, 1999
Max Planck Institute for Meteorology, Germany	ECHAM5/ MPI-OM	1...3	1...3	1...3	Jungclaus et al., 2006
Meteorological Research Institute, Japan	MRI-CGCM2.3.2	1...5	1...5	1...5	Yukimoto et al., 2001
National Center for Atmospheric Research, USA	CCSM3	1...4	1...3, 5...7	1...7	Collins et al., 2006
National Center for Atmospheric Research, USA	PCM	1...4	1...4	2...3	Washington et al., 2000
Hadley Centre for Climate Prediction and Research/Met Office, UK	UKMO-HadCM3	1	1	1	Gordon et al., 2000

3.2 Bias Correction and Downscaling

The CMIP3 climate projections have been bias corrected and spatially downscaled to one-eighth-degree (~12-kilometer) resolution through methods described in detail in Wood et al. (2002), Wood et al. (2004), and Maurer (2007). The purpose of bias correction is to adjust a given climate projection for inconsistencies between the simulated historical climate data and observed historical climate data, which are the result of GCM bias. In the BCSD approach, projections are bias-corrected using a quantile mapping technique. Following bias correction, the adjusted climate projection data are statistically consistent with the observed climate data for the historical overlap period, which is 1950 to 1999 in the Study. Beyond the historical overlap period (i.e., 2000 to 2099), the adjusted climate projection data reflect the same relative changes in mean, variance, and other statistics between the future (2000 to 2099) and historical periods (1950 to 1999) as was present in the unadjusted dataset, but the adjusted climate projection data are mapped onto the observed dataset variance. Note that this methodology assumes that the GCM biases have the same structure during the 20th and 21st-centuries' simulations.

Downscaling spatially translates bias corrected climate data from the coarse, 2-degree (~200-kilometer), spatial resolution typical of climate models to a basin-relevant resolution of one-eighth-degree (12-kilometer), which is more useful for hydrology and other applications. The spatial downscaling process generally preserves observed spatial relationships between large- and fine-scale climate. This approach assumes that the topographic and climatic features that determine the fine-scale distribution of large-scale climate will be the same in the future as in the historical record.

3.2.1 Gridded Climate Dataset Description

Each of the 112 bias-corrected and spatially downscaled climate projections included in the CMIP3 dataset includes the following two parameters: (1) mean daily rate of precipitation for each month (mm/day) and (2) mean monthly surface air temperature (°C). The projection data spans from 1950 to 2099 on a monthly time step, for a total of 1,800 time steps. The spatial coverage of the data includes the contiguous U.S. and small portions of southern Canada and northern Mexico (25.125° N to 52.875° N and 124.625° W to 67.000° W). The resolution of the dataset is one-eighth-degree, or approximately 12 by 12 kilometers. The climate projection data are stored in the netCDF file format.

3.2.2 Hydrologic Modeling

Using a quantile mapping process, the bias-corrected spatially downscaled CMIP3 dataset were converted to the appropriate input format for the VIC hydrologic model. Developed at the University of Washington, the VIC model is a semi-distributed macro-scale hydrologic model that solves the water balance at each model grid cell. A VIC model of the Colorado River Basin was previously developed by the University of Washington (Christensen and Lettenmaier, 2009). This model was provided to Reclamation for the purpose of further calibration and analysis, and all operation of the model for the Study was conducted by the subconsultant, AMEC. In addition to producing routed streamflows at specified locations, the VIC model also provides output for the hydrologic process indicators, including precipitation, runoff, baseflow, evapotranspiration (ET), soil moisture, and SWE. Appendix B4 provides further discussion of the VIC model.

3.2.3 Climate and Gridded Hydrologic Process Analysis Methods

Gridded climate and hydrologic process data were generated by the VIC model for the historical and the 112 climate projection scenarios. These data were converted to a specialized format, allowing for statistical analysis and visualization via spatial mapping. This analysis was performed to better understand the primary factors, both climatological and hydrological, that drive projected changes in streamflows relative to historical conditions.

3.2.4 Production of Gridded Data Sets

VIC Model Flux Files

In addition to streamflows, the VIC model exports climate and hydrologic data for each simulation. The climate data include average air temperature (°C) generated during the model simulations and precipitation (millimeters), which is consistent with the data provided in the model input files. Hydrologic parameters include ET, runoff (surface runoff), baseflow (subsurface runoff), soil moisture (in each of three soil layers), and SWE. Both the climate and hydrologic data are stored in ASCII formatted text files known as "flux files." One flux file is produced for every grid cell of the study area, and each file contains values for the specified parameters at every time step of the simulation. A summary of flux file parameters is as follows:

Climatological Parameters	Hydrologic Parameters
Average air temperature (°C)	Soil moisture (three layers) (millimeters)
Precipitation (millimeters)	SWE (millimeters)
	ET (millimeters)
	Runoff (surface) (millimeters)
	Baseflow (subsurface) (millimeters)

Conversion of Flux File Data to netCDF

The flux file output generated by the VIC model was converted to network Common Data Form (netCDF) to more readily evaluate and visualize the data. Developed by staff at the Unidata Program Center in Boulder, Colorado, netCDF is a machine-independent data format for array-oriented (i.e., multi-dimensional) scientific data. In particular, netCDF is well suited to spatially gridded time series data, such as gridded climate data. Unidata has developed a variety of software libraries and tools that support the creation, manipulation, and analysis of multi-dimensional data. Unidata's netCDF-Java library was used to develop an application-specific Java program to convert the VIC flux files from ASCII format to netCDF format.

The resulting netCDF files are each three-dimensional (3D), defined by latitude, longitude, and time. The spatial extent of the hydrologic basin spans from 31.3125°N to 43.4375°N and from 115.6875°W to 105.6875°W. Given a grid cell size of one-eighth degree, the latitude dimension spans 98 grid cells, while the longitude dimension spans 81 grid cells, for a total 7,938 grid cells. The temporal extent of the data is from 1950 to 2099. Given a monthly time step, the time dimension consists of 1,800 values.

Each netCDF file contains data for 13 climate and hydrologic parameters. Some analysis was conducted during the file conversion process to generate time series of new and meaningful parameters for the netCDF output files. New parameters include the following:

- ET Efficiency: the ratio of actual ET to potential ET (percent)
- Total Runoff: the sum of runoff (surface) and baseflow (subsurface runoff) (millimeters)
- Total Runoff Efficiency: The ratio of runoff to precipitation (percent)
- Soil Moisture Sum: The sum of the soil moisture for all three soil layers (millimeters)
- Maximum Soil Moisture: The maximum soil moisture possible for all three soil layers (millimeters)
- Soil Moisture Fraction: The ratio of the soil moisture sum to the maximum soil moisture (percent)

The complete list of parameters included in the netCDF files is as follows:

- Average air temperature (°C)
- Precipitation (millimeters)
- ET (millimeters)
- Potential ET (millimeters)
- ET Efficiency (percent)
- Runoff (surface) (millimeters)
- Baseflow (subsurface) (millimeters)
- Total Runoff (millimeters)
- Total Runoff Efficiency (percent)
- Soil Moisture Sum (millimeters)
- Maximum Soil Moisture (millimeters)
- Soil Moisture Fraction (percent)
- SWE (millimeters)

One netCDF file was produced for each climate projection and for the historic scenario, for a total of 113 netCDF files.

3.3 Statistical Analysis

To quantify potential changes between historical and future time periods, the VIC output data were statistically evaluated. For each historical and future time period of interest, statistics were developed for the consolidated dataset consisting of all 112 projections, such that the resulting statistics are representative of the 112-member ensemble. Statistics were generated for a subset of the VIC output parameters and derived parameters described previously. The eight parameters evaluated are as follows:

- Average air temperature (°C)
- Precipitation (millimeters)
- ET (millimeters)
- ET Efficiency (percent)
- Total Runoff (millimeters)
- Total Runoff Efficiency (percent)
- Soil Moisture Fraction (percent)
- SWE (millimeters)

A Java program was developed to process the VIC model output data stored in the netCDF files described previously. The Java program relies heavily on the netCDF-Java library, and on the *Descriptive Statistics* package of the Apache Commons math library. The statistics generated for each parameter include the mean, standard deviation, variance, skewness, minimum, and maximum. In addition, the cumulative distribution function (CDF) for each time period was produced. A CDF describes the probability that a data point will be found at a value less than or equal to some value, "*x*." For this analysis, "*x*" values corresponding to all integer percentiles from 1 to 100 (inclusive) were generated for each CDF.

3.3.1 Analysis Time Periods

Three future periods were selected for comparison to the historical period. Each period, including the historical, consists of 30 years and is identified by the representative middle value that defines that period. For example, the historical period consists of the years 1971 to 2000, and is represented by the year 1985. The historical period of 1971 to 2000 is selected as the reference climate since it is the currently established climate normal used by NOAA and represents the most recent time period The three future periods selected for analysis were 2011 to 2040 (represented by the year 2025), 2041 to 2070 (represented by the year 2055), and 2066 to 2095 (represented by the year 2080). The last year of the climate projections is 2099, which is one year short of a 30-year period starting in 2071. Therefore, the end year for the 2080 period was selected to be 2095. Thus, the 2080 period includes five years of overlap (2066-2070) with the 2055 period. For each of the four time periods specified, the representative statistics described previously were generated on a monthly, seasonal, and annual basis. In this analysis, the seasons are defined as follows:

- Fall: OND
- Winter: JFM
- Spring: AMJ
- Fall: JAS

3.3.2 Analysis Spatial Scale

The statistical analysis described previously was conducted on both a grid cell and watershed basis. The results of the grid cell analysis produce the most informative map graphics and clearly show spatial variation at the greatest resolution possible. At this spatial scale, the statistics for each grid cell are developed independently.

In contrast, watershed statistics are developed concurrently for all grid cells that are members of a watershed unit. In this case, a time series of watershed data is generated for each parameter prior to conducting the statistical analysis. For a given watershed, this is done by averaging the values of all member grid cells for each time step of the simulation period. The statistical analysis is then applied to the watershed time series, such that the resulting values are representative of the watershed as a whole. The watershed analysis results in a more manageable set of outputs and is useful for evaluating trends in different regions of the basin.

3.3.3 Statistical Analysis Output

The resulting statistics are stored in 4-dimensional (4D) netCDF files, which are defined by latitude, longitude, time, and statistic. The spatial extent of the study area spans from 31.3125°N to 43.4375°N and from 115.6875°W to 105.6875°W. Given a grid cell size of one-eighth degree,

the latitude dimension spans 98 grid cells, while the longitude dimension spans 81 grid cells, for a total 7,938 grid cells. The temporal "extent" of the data consists of 17 values, each of which represents a monthly (1 to 12), annual (13), or seasonal (14 to 17) analysis time. The "statistic" dimension contains 111 values. The first 100 values are integer percentiles corresponding to the CDF distribution. The last 11 values represent the general statistics—mean, standard deviation, variance, skewness, minimum, P10, P25, P50, P75, P90, and maximum. Two netCDF files are produced for each of the four time periods—one for the grid cell based statistics and one for the watershed based statistics. Each netCDF file contains statistics representative of the 112-member projection ensemble for each of the eight climatological and hydrologic parameters identified previously. For watershed statistics, text files containing the general statistics and CDF values are also produced for each variable and time period. This output allows for ready production of spreadsheet charts, such as those presented in the results section.

3.3.4 Change Metrics

Finally, "change metrics" are generated for each parameter in which the difference between future period statistics and historical period statistics are calculated on both absolute and percent change bases. These results are again stored in netCDF files, with two files generated for each future period—one for grid cell data and one for watershed data. The format of these files is identical to those containing the results of the statistical analysis.

Appendix B6
Streamflow Analysis

Appendix B6—Streamflow Analysis

1.0 Streamflow Data Source

The streamflow analysis was based on reconstructed natural flows in the Basin. The data consists of two historical datasets. The first dataset (referred to as the observed record) consists of monthly observed natural flows for the period October 1905 to September 2007. The second dataset (referred as the paleo record) consists of monthly flows reconstructed from tree ring analysis for the period October 761 to September 2005.

The observed record was provided in the total flows format (flows accumulating from upstream to downstream locations) and intervening format (single watershed flows). The original paleo record was originally in the single format and had to be accumulated from upstream to downstream basins to a total flows format.

Streamflow analyses were also performed for streamflows originated from the VIC hydrology model (referred as downscaled GCM projected streamflows). The analyses were similar to the analyses performed for the observed and paleo records; however, different since several realizations from multiple GCMs, greenhouse gas emission scenarios and initial conditions are available.

2.0 Streamflow Data Summary

Streamflows were analyzed for the 29 natural flow stations that serve as the primary inflow locations for CRSS. A spreadsheet tool was constructed to provide an interactive environment to explore the temporal and spatial characteristics of streamflow in the Basin as shown in Figure B6-1. The features of this visual summary are described as follows.

FIGURE B6-1

Summary Graphic for Colorado River at Lees Ferry Displaying Streamflow, Annual Exceedance Probabilities, Streamflow Deficits and Surpluses, and Drought Duration, Magnitude and Intensity

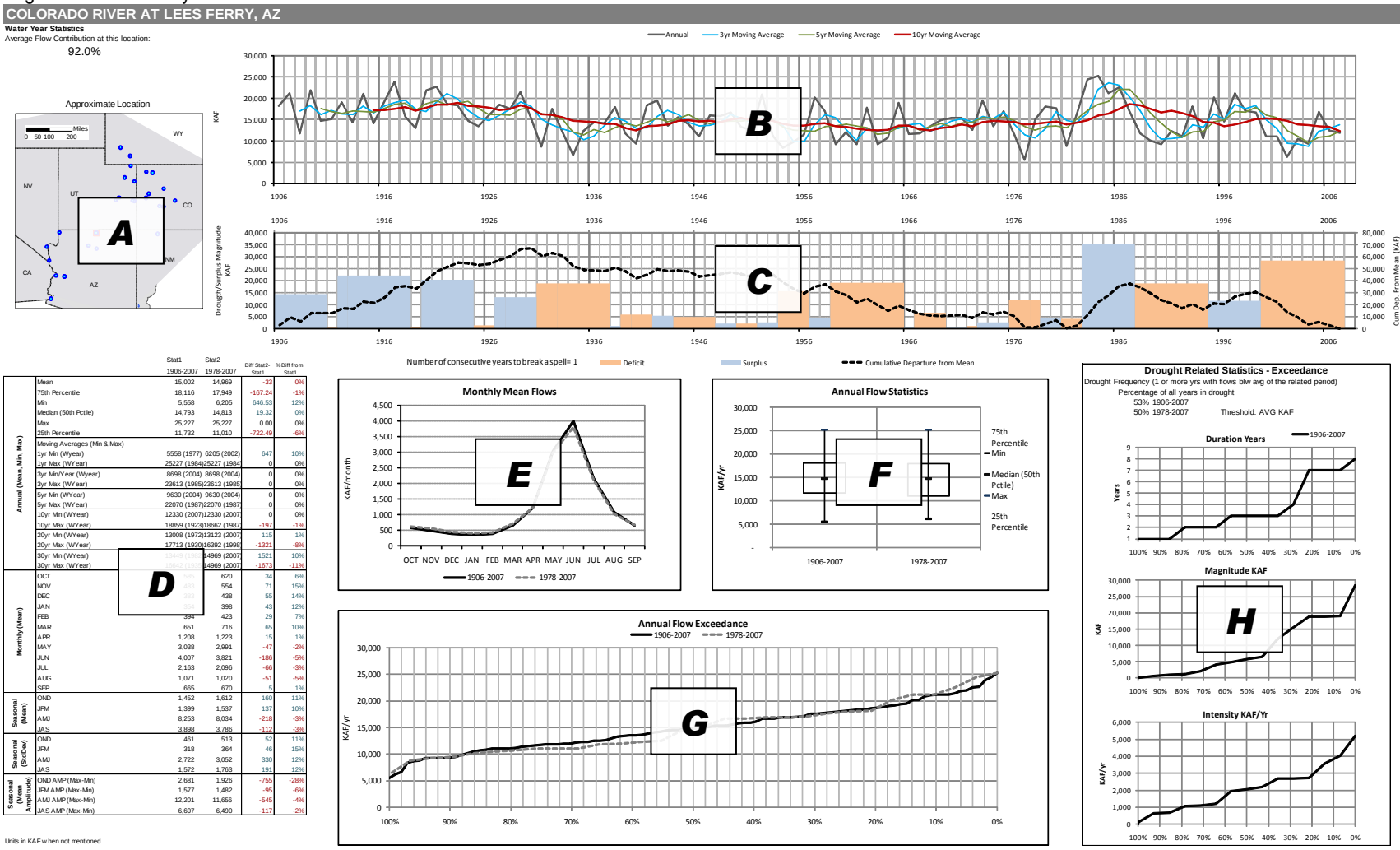

A. Streamflow Location: The approximate location of the flow station being summarized in the spreadsheet within the Basin.

B. Observed Annual Streamflow Graphic: A time series plot of volume in thousands of acre-feet (KAF) for the selected location. This chart also shows the 5, 10, 20, and 30 year moving averages for annual streamflow.

C. Deficit/Surplus Evaluation Graphic: This dual-axis plot displays deficits and surpluses (colored vertical bars) based on the long-term average of 15 maf and accumulated streamflows (dashed black line) based on the long-term average. The left axis provides the scale for the colored vertical bars and the right axes provides the scale for the dashed line. The vertical bars represent periods of uninterrupted deficit or surplus. The width of the bar indicates the number of years of uninterrupted deficit or surplus and the height indicates the magnitude of the accumulated deficit or surplus. The values were computed by evaluating how long annual flows would be below (deficit) or above (surplus) the long-term average.. The dashed line provides a streamflow rate of change indicator; the greater the slope, the greater the rate of change in accumulated flows from the long-term average.

D. Table of Statistics: The table includes statistics (Stat1 and Stat2) for two periods in columns that represent the absolute and percentage difference between the two time periods. The Stat1 and Stat2 columns present the long-term water year streamflow average for the two periods. The "Annual" statistic block shows the minimum and the maximum observed for the 1-year totals and 5, 10, 20, and 30 year moving averages followed by the year that the value was observed (e.g. the line "3yr Min/Year 7370/1847" represents a minimum value of 7370 KAF per year for a 3-year moving average time series ending in the year of 1847). The "Averages per month" section shows the monthly streamflow averages for each month followed by the seasonal statistics (average, standard deviation, and amplitude [maximum-minimum]). The amplitude accounts for all seasons, for example, for amplitude OND, the value on the table is computed as the maximum flow observed in a OND season minus the minimum flow observed in a OND season. The minimum and the maximum do not necessarily occur in the same water year.

E. Average Monthly Streamflow Graphic: Average monthly streamflow (KAF) is shown for the water year over the time periods. The data used for this plot are also presented in the Table of Statistics as Stat1 (solid line) and Stat2 (dashed line). This graphic can be used to assess monthly and seasonal shifts in streamflow from the comparison periods.

F. Annual Streamflow Box and Whiskers Graphic: This plot illustrates annual streamflow variability for the two time periods. The box represents the range of half of annual observed flows (inter-quartile range between 25^{th} and 75^{th} percentile). The triangle represents the median, the diamonds represent the 25 and 75 percent exceedance values, and the horizontal lines at the top of the vertical line represent the period of record maximum and minimum annual values. This graphic can be used to assess trends in period streamflow variability and volumes.

G. Annual Streamflow Exceedance Graphic: This plot presents the full range of probabilities of exceeding a given streamflow for two selected periods. The plot is equivalent to the Box and Whiskers plot but provides probabilities ranging from zero to 100 percent. This graphic can be used to assess trends in period streamflow variability and volumes. For example, at the

Lees Ferry location, 90 percent of the years had streamflows exceeding 10,000 KAF for both periods.

H. Deficit Related Statistics – Exceedance Plots: The deficit statistics are illustrated in three charts: duration, magnitude, and intensity. The statistics presented in these charts refer only to deficit periods defined as only the years when streamflows were below the specified threshold. The "percentage of all years in a deficit" takes into account all years in the time period and determines how many were within a "deficit". Below there is a more detailed description of the deficit related statistics.

   The average streamflow for each time period is the default threshold to define deficit or surplus periods (e.g., a sequence of years with streamflows below the average will be considered a deficit period).

   Duration: The duration chart presents the exceedance probability of deficit duration in years. For example, the chart illustrates that at Lees Ferry, 30 percent of the years defined as deficit years (only deficit years) had a deficit that lasted or exceeded 3 years in duration.

   Magnitude: The magnitude of a deficit (in KAF) corresponds to the cumulative difference between observed streamflows and long-term average streamflows for an uninterrupted drought period. The exceedance plot will show the probability of a deficit to exceed a certain magnitude based on observed flows.

   Intensity: Deficit intensity is presented as magnitude divided by duration. The chart presents the exceedance probabilities for two selected periods.

3.0 Streamflow Data Summaries

Sample streamflow data summaries are provided in the following pages. The full summaries are included for the following natural flow stations:

Figure B6-2. Colorado River at Lees Ferry (Station 20)
Figure B6-3. Green River at Green River UT (Station 16)
Figure B6-4. Colorado River Near Cisco (Station 8)
Figure B6-5. San Juan River near Bluff (Station 19)
Figure B6-6. Colorado River at Imperial Dam (Station 29)

Additional locations could be added in the future.

FIGURE B6-2

Streamflow Data Summary for Colorado River at Lees Ferry Natural Flows (Based on historical 1906-2007 data)

COLORADO RIVER AT LEES FERRY, AZ

Water Year Statistics

Average Flow Contribution at this location:

92.0%

Approximate Location

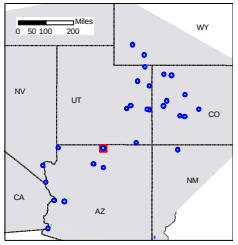

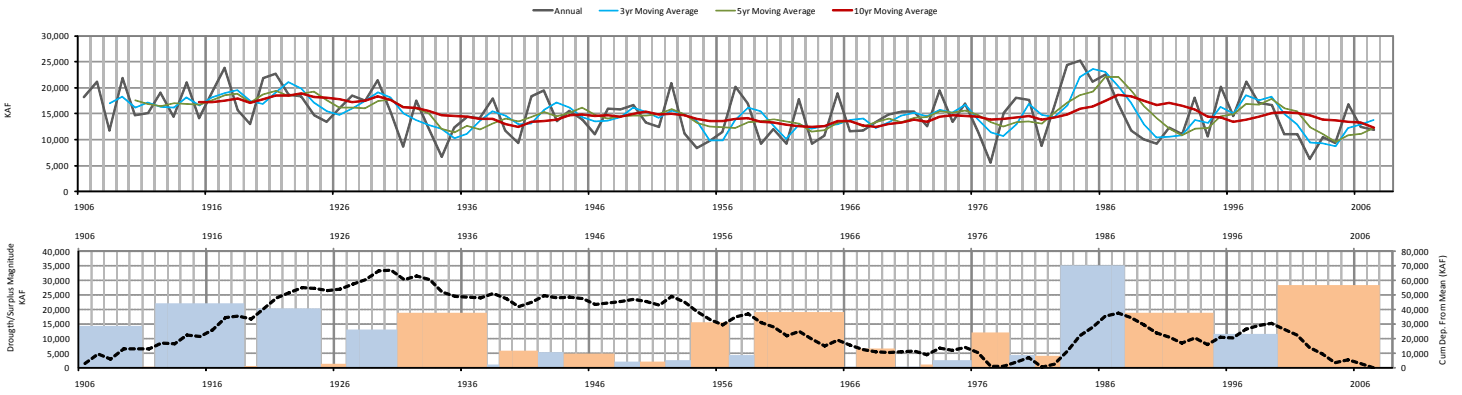

		Stat1 1906-2007	Stat2 1978-2007	Diff Stat2-Stat1	%Diff from Stat1
Annual (Mean, Min, Max)	Mean	15,002	14,969	-33	0%
	75th Percentile	18,116	17,949	-167.24	-1%
	Min	5,558	6,205	646.53	12%
	Median (50th Pctile)	14,793	14,813	19.32	0%
	Max	25,227	25,227	0.00	0%
	25th Percentile	11,732	11,010	-722.49	-6%
	Moving Averages (Min & Max)				
	1yr Min (Wyear)	5558 (1977)	6205 (2002)	647	10%
	1yr Max (WYear)	25227 (1984)	25227 (1984)	0	0%
	3yr Min/Year (Wyear)	8698 (2004)	8698 (2004)	0	0%
	3yr Max (WYear)	23613 (1985)	23613 (1985)	0	0%
	5yr Min (WYear)	9630 (2004)	9630 (2004)	0	0%
	5yr Max (WYear)	22070 (1987)	22070 (1987)	0	0%
	10yr Min (WYear)	12330 (2007)	12330 (2007)	0	0%
	10yr Max (WYear)	18859 (1923)	18662 (1987)	-197	-1%
	20yr Min (WYear)	13008 (1972)	13123 (2007)	115	1%
	20yr Max (WYear)	17713 (1930)	16392 (1998)	-1321	-8%
	30yr Min (WYear)	13449 (1982)	14969 (2007)	1521	10%
	30yr Max (WYear)	16642 (1935)	14969 (2007)	-1673	-11%
Monthly (Mean)	OCT	585	620	34	6%
	NOV	483	554	71	15%
	DEC	383	438	55	14%
	JAN	354	398	43	12%
	FEB	394	423	29	7%
	MAR	651	716	65	10%
	APR	1,208	1,223	15	1%
	MAY	3,038	2,991	-47	-2%
	JUN	4,007	3,821	-186	-5%
	JUL	2,163	2,096	-66	-3%
	AUG	1,071	1,020	-51	-5%
	SEP	665	670	5	1%
Seasonal (Mean)	OND	1,452	1,612	160	11%
	JFM	1,399	1,537	137	10%
	AMJ	8,253	8,034	-218	-3%
	JAS	3,898	3,786	-112	-3%
Seasonal (StdDev)	OND	461	513	52	11%
	JFM	318	364	46	15%
	AMJ	2,722	3,052	330	12%
	JAS	1,572	1,763	191	12%
Seasonal (Mean Amplitude)	OND AMP (Max-Min)	2,681	1,926	-755	-28%
	JFM AMP (Max-Min)	1,577	1,482	-95	-6%
	AMJ AMP (Max-Min)	12,201	11,656	-545	-4%
	JAS AMP (Max-Min)	6,607	6,490	-117	-2%

Units in KAF when not mentioned

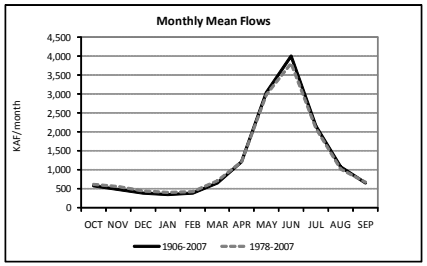

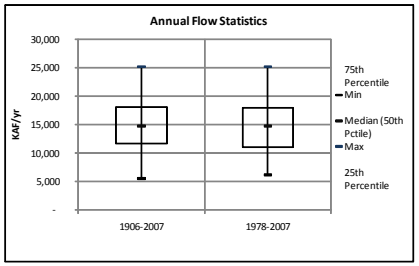

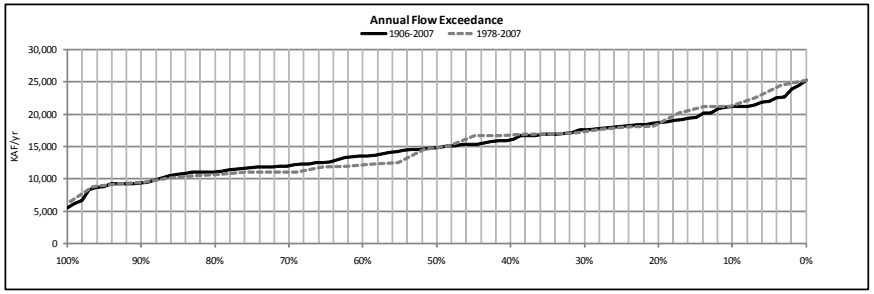

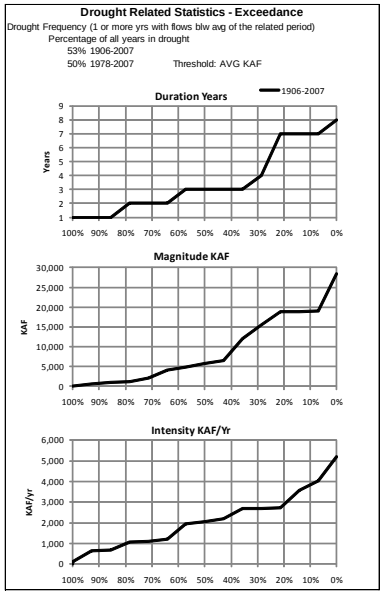

Colorado River Water Supply Analysis

FIGURE B6-3

Streamflow Data Summary for Green River at Green River, UT Natural Flows (Based on historical 1906-2007 data)

GREEN RIVER AT GREEN RIVER, UT

Water Year Statistics

Average Flow Contribution at this location:

33.0%

Approximate Location

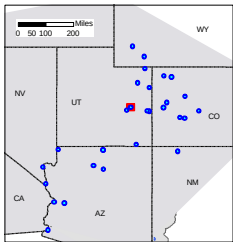

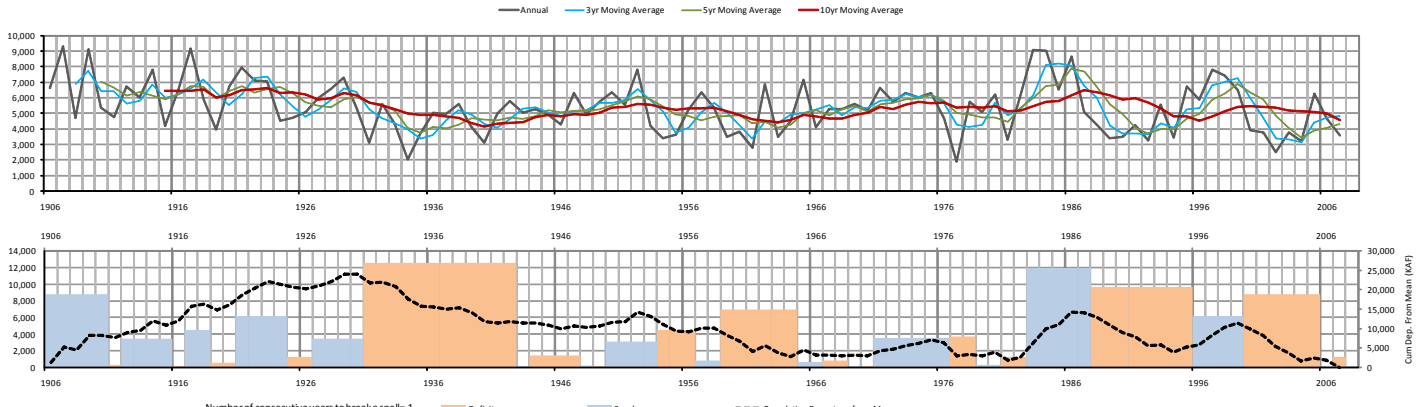

		Stat1 1906-2007	Stat2 1978-2007	Diff Stat2-Stat1	%Diff from Stat1
Annual (Mean, Min, Max)	Mean	5,385	5,288	-97	-2%
	75th Percentile	6,360	6,451	90.95	1%
	Min	1,903	2,515	612.21	32%
	Median (50th Pctile)	5,284	5,091	-192.75	-4%
	Max	9,297	9,076	-221.42	-2%
	25th Percentile	4,192	3,642	-549.81	-13%
	Moving Averages (Min & Max)				
	1yr Min (Wyear)	1903 (1977)	2515 (2002)	612	24%
	1yr Max (WYear)	9297 (1907)	9076 (1983)	-221	-2%
	3yr Min/Year (Wyear)	3161 (2004)	3161 (2004)	0	0%
	3yr Max (WYear)	8210 (1985)	8210 (1985)	0	0%
	5yr Min (WYear)	3434 (2004)	3434 (2004)	0	0%
	5yr Max (WYear)	7897 (1986)	7897 (1986)	0	0%
	10yr Min (WYear)	4174 (1940)	4528 (1996)	354	8%
	10yr Max (WYear)	6639 (1923)	6497 (1987)	-142	-2%
	20yr Min (WYear)	4684 (2007)	4684 (2007)	0	0%
	20yr Max (WYear)	6417 (1925)	5803 (1999)	-614	-11%
	30yr Min (WYear)	4800 (1961)	5288 (2007)	488	9%
	30yr Max (WYear)	5913 (1935)	5288 (2007)	-625	-12%
Monthly (Mean)	OCT	183	202	18	10%
	NOV	156	172	16	10%
	DEC	117	127	9	8%
	JAN	120	131	11	10%
	FEB	142	155	13	9%
	MAR	292	312	20	7%
	APR	485	478	-6	-1%
	MAY	1,127	1,118	-10	-1%
	JUN	1,432	1,348	-84	-6%
	JUL	751	687	-65	-9%
	AUG	370	349	-21	-6%
	SEP	208	210	2	1%
Seasonal (Mean)	OND	457	501	43	9%
	JFM	554	598	44	8%
	AMJ	3,044	2,944	-100	-3%
	JAS	1,330	1,246	-84	-6%
Seasonal (Std/Dev)	OND	146	190	44	30%
	JFM	148	146	-1	-1%
	AMJ	1,049	1,184	135	13%
	JAS	547	563	16	3%
Seasonal (Mean Amplitude)	OND AMP (Max-Min)	774	638	-136	-18%
	JFM AMP (Max-Min)	712	607	-105	-15%
	AMJ AMP (Max-Min)	4,560	3,996	-563	-12%
	JAS AMP (Max-Min)	2,744	1,943	-802	-29%

Units in KAF when not mentioned

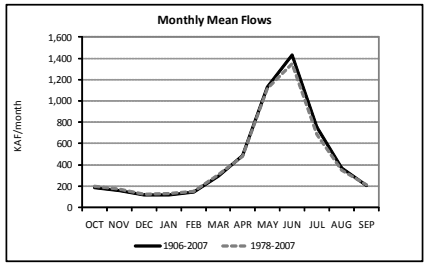

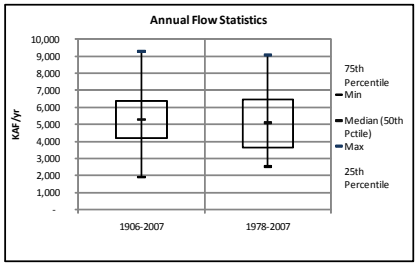

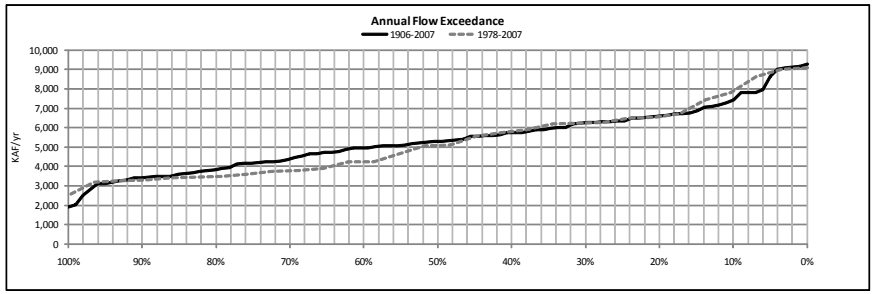

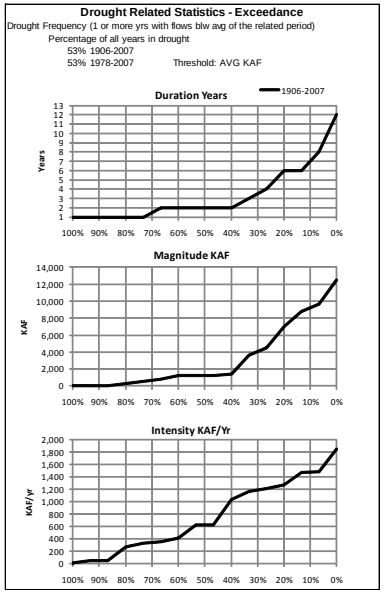

Colorado River Water Supply Analysis

FIGURE B6-4

Streamflow Data Summary for Colorado River near Cisco, UT Natural Flows (Based on historical 1906-2007 data)

COLORADO RIVER NEAR CISCO, UT

Water Year Statistics

Average Flow Contribution at this location:

41.6%

Approximate Location

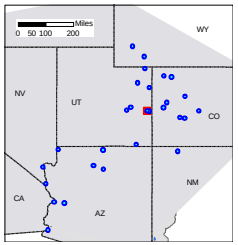

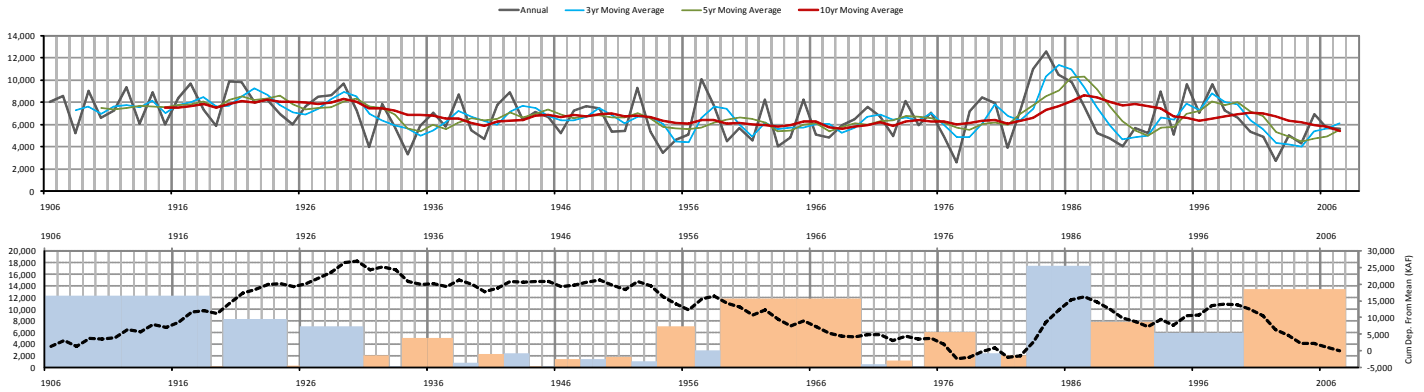

		Stat1 1906-2007	Stat2 1978-2007	Diff Stat2-Stat1	%Diff from Stat1
Annual (Mean, Min, Max)	Mean	6,793	6,869	76	1%
	75th Percentile	8,196	8,306	110.88	1%
	Min	2,625	2,702	76.78	3%
	Median (50th Pctile)	6,842	6,759	-83.32	-1%
	Max	12,561	12,561	0.00	0%
	25th Percentile	5,241	5,140	-101.08	-2%
	Moving Averages (Min & Max)				
	1yr Min (Wyear)	2625 (1977)	2702 (2002)	77	3%
	1yr Max (WYear)	12561 (1984)	12561 (1984	0	0%
	3yr Min/Year (Wyear)	3996 (2004)	3996 (2004)	0	0%
	3yr Max (WYear)	11347 (1985)	11347 (1985)	0	0%
	5yr Min (WYear)	4448 (2004)	4448 (2004)	0	0%
	5yr Max (WYear)	10314 (1987)	10314 (1987	0	0%
	10yr Min (WYear)	5431 (2007)	5431 (2007)	0	0%
	10yr Max (WYear)	8636 (1987)	8636 (1987)	0	0%
	20yr Min (WYear)	5875 (1978)	5985 (2007)	110	2%
	20yr Max (WYear)	7972 (1930)	7590 (1998)	-382	-5%
	30yr Min (WYear)	6046 (1978)	6869 (2007)	823	12%
	30yr Max (WYear)	7457 (1935)	6869 (2007)	-589	-9%
Monthly (Mean)	OCT	255	271	16	6%
	NOV	214	240	26	12%
	DEC	178	198	20	11%
	JAN	163	175	12	7%
	FEB	157	164	7	5%
	MAR	224	253	29	13%
	APR	533	556	24	4%
	MAY	1,516	1,517	1	0%
	JUN	1,875	1,786	-90	-5%
	JUL	940	954	14	2%
	AUG	455	462	7	2%
	SEP	283	293	10	3%
Seasonal (Mean)	OND	646	709	62	10%
	JFM	544	591	48	9%
	AMJ	3,924	3,859	-65	-2%
	JAS	1,678	1,710	31	2%
Seasonal (StdDev)	OND	161	197	36	22%
	JFM	106	138	32	30%
	AMJ	1,317	1,571	255	19%
	JAS	665	788	123	18%
Seasonal (Mean Amplitude)	OND AMP (Max-Min)	845	740	-105	-12%
	JFM AMP (Max-Min)	611	590	-21	-3%
	AMJ AMP (Max-Min)	6,563	6,495	-68	-1%
	JAS AMP (Max-Min)	3,154	3,071	-83	-3%

Units in KAF when not mentioned

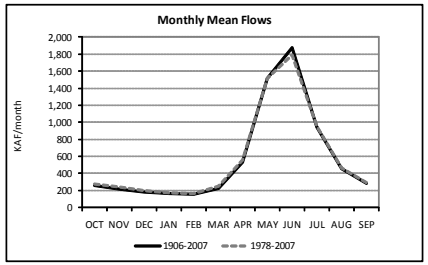

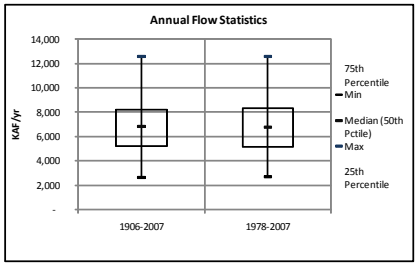

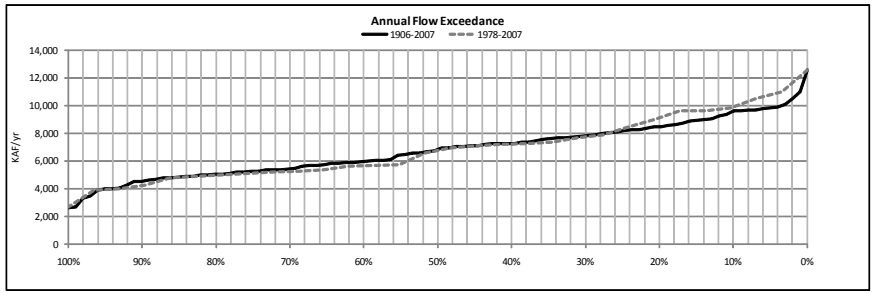

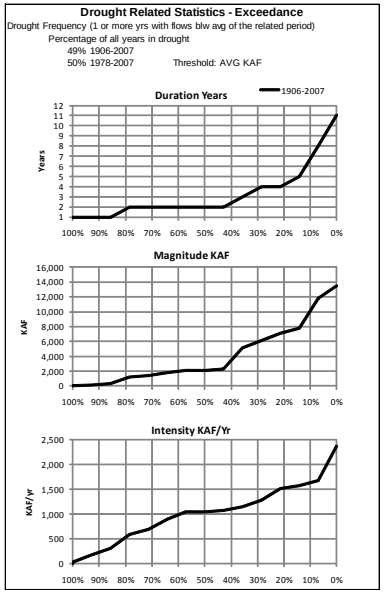

Colorado River Water Supply Analysis

FIGURE B6-5

Streamflow Data Summary for San Juan River near Bluff, UT Natural Flows (Based on historical 1906-2007 data)

SAN JUAN RIVER NEAR BLUFF, UT

Water Year Statistics

Average Flow Contribution at this location:

13.1%

Approximate Location

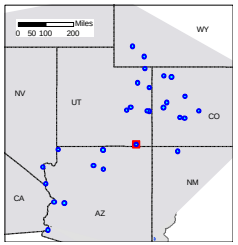

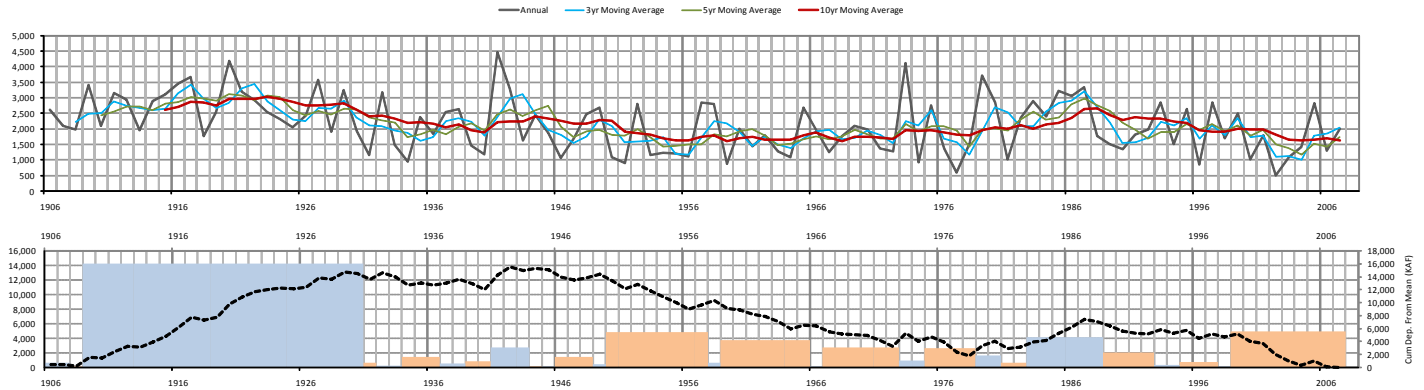

		Stat1 1906-2007	Stat2 1978-2007	Diff Stat2-Stat1	%Diff from Stat1
Annual (Mean, Min, Max)	Mean	2,139	2,060	-79	-4%
	75th Percentile	2,830	2,841	11.24	0%
	Min	514	514	0.00	0%
	Median (50th Pctile)	1,987	1,899	-87.43	-4%
	Max	4,466	3,718	-748.01	-17%
	25th Percentile	1,380	1,451	70.73	5%
	Moving Averages (Min & Max)				
	1yr Min (Wyear)	514 (2002)	514 (2002)	0	0%
	1yr Max (WYear)	4466 (1941)	3718 (1979)	-748	-20%
	3yr Min/Year (Wyear)	1011 (2004)	1011 (2004)	0	0%
	3yr Max (WYear)	3438 (1922)	3214 (1987)	-223	-7%
	5yr Min (WYear)	1170 (2004)	1170 (2004)	0	0%
	5yr Max (WYear)	3127 (1920)	2986 (1987)	-141	-5%
	10yr Min (WYear)	1603 (1959)	1620 (2007)	17	1%
	10yr Max (WYear)	3032 (1923)	2666 (1988)	-366	-14%
	20yr Min (WYear)	1663 (1972)	1769 (2007)	106	6%
	20yr Max (WYear)	2811 (1927)	2288 (1998)	-522	-23%
	30yr Min (WYear)	1732 (1972)	2060 (2007)	328	19%
	30yr Max (WYear)	2584 (1938)	2060 (2007)	-524	-25%
Monthly (Mean)	OCT	101	94	-7	-7%
	NOV	64	73	10	15%
	DEC	51	57	6	12%
	JAN	50	58	8	15%
	FEB	69	74	5	8%
	MAR	123	146	23	19%
	APR	248	264	16	7%
	MAY	453	453	0	0%
	JUN	481	447	-34	-7%
	JUL	233	181	-52	-22%
	AUG	150	113	-36	-24%
	SEP	117	99	-18	-15%
Seasonal (Mean)	OND	216	224	9	4%
	JFM	242	278	36	15%
	AMJ	1,182	1,164	-18	-2%
	JAS	500	394	-106	-21%
Seasonal (StdDev)	OND	139	106	-33	-24%
	JFM	111	127	16	14%
	AMJ	548	561	13	2%
	JAS	288	219	-69	-24%
Seasonal (Mean Amplitude)	OND AMP (Max-Min)	886	522	-364	-41%
	JFM AMP (Max-Min)	472	435	-37	-8%
	AMJ AMP (Max-Min)	2,631	2,440	-190	-7%
	JAS AMP (Max-Min)	1,349	872	-476	-35%

Units in KAF when not mentioned

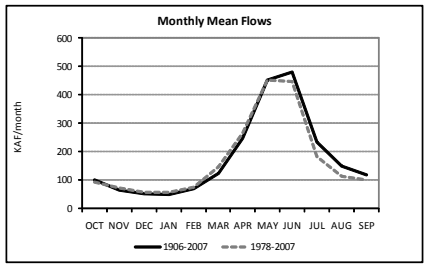

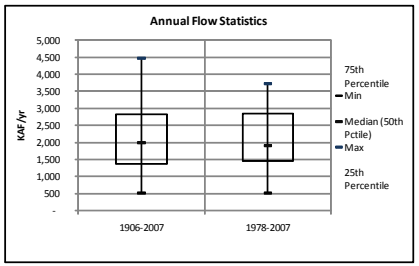

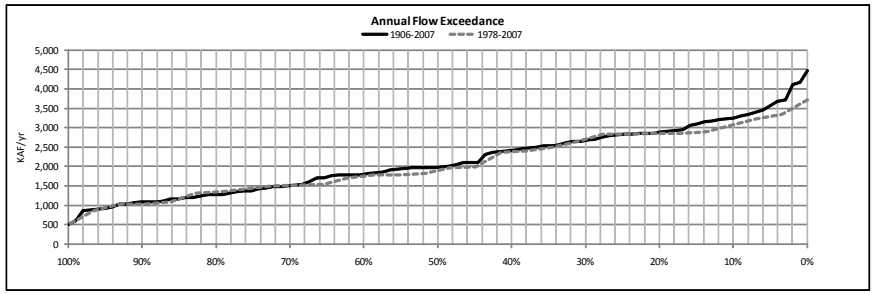

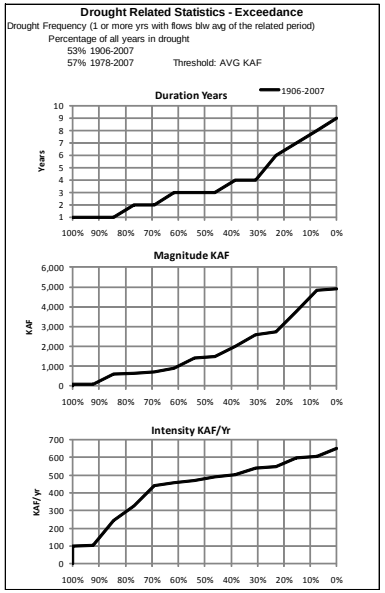

Colorado River Water Supply Analysis

FIGURE B6-6

Streamflow Data Summary for Colorado River above Imperial Dam Natural Flows (Based on historical 1906-2007 data)

COLORADO RIVER ABOVE IMPERIAL DAM, AZ-CA

Water Year Statistics

Average Flow Contribution at this location:

100.0%

Approximate Location

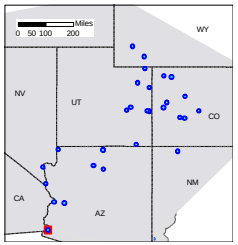

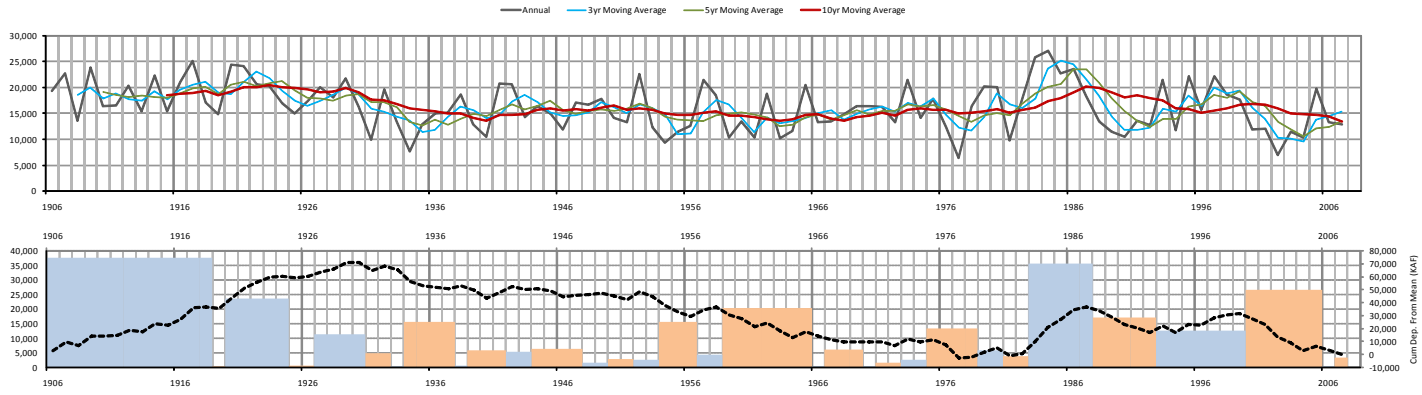

		Stat1 1906-2007	Stat2 1978-2007	Diff Stat2-Stat1	%Diff from Stat1
Annual (Mean, Min, Max)	Mean	16,311	16,394	83	1%
	75th Percentile	20,058	20,154	95.85	0%
	Min	6,377	6,914	536.44	8%
	Median (50th Pctile)	16,311	16,035	-275.71	-2%
	Max	27,090	27,090	0.00	0%
	25th Percentile	12,899	11,968	-931.14	-7%
	Moving Averages (Min & Max)				
	1yr Min (Wyear)	6377 (1977)	6914 (2002)	536	8%
	1yr Max (WYear)	27090 (1984)	27090 (1984	0	0%
	3yr Min/Year (Wyear)	9562 (2004)	9562 (2004)	0	0%
	3yr Max (WYear)	25199 (1985)	25199 (1985)	0	0%
	5yr Min (WYear)	10542 (2004)	10542 (2004	0	0%
	5yr Max (WYear)	23513 (1987)	23513 (1987	0	0%
	10yr Min (WYear)	13487 (2007)	13487 (2007	0	0%
	10yr Max (WYear)	20524 (1923)	20215 (1987	-309	-2%
	20yr Min (WYear)	14224 (1972)	14484 (2007	260	2%
	20yr Max (WYear)	19265 (1925)	17956 (1998	-1309	-7%
	30yr Min (WYear)	14700 (1978)	16394 (2007	1694	10%
	30yr Max (WYear)	18080 (1935)	16394 (2007	-1686	-10%
Monthly (Mean)	OCT	691	746	55	8%
	NOV	543	642	99	18%
	DEC	455	526	71	16%
	JAN	417	503	85	20%
	FEB	495	555	61	12%
	MAR	756	857	102	13%
	APR	1,312	1,335	23	2%
	MAY	3,109	3,098	-11	0%
	JUN	4,118	3,886	-232	-6%
	JUL	2,355	2,226	-129	-5%
	AUG	1,249	1,199	-50	-4%
	SEP	812	821	9	1%
Seasonal (Mean)	OND	1,688	1,914	226	13%
	JFM	1,667	1,915	248	15%
	AMJ	8,539	8,319	-220	-3%
	JAS	4,417	4,246	-170	-4%
Seasonal (StdDev)	OND	515	533	19	4%
	JFM	501	612	111	22%
	AMJ	2,786	3,105	319	11%
	JAS	1,619	1,808	189	12%
Seasonal (Mean Amplitude)	OND AMP (Max-Min)	2,491	1,937	-555	-22%
	JFM AMP (Max-Min)	2,892	2,646	-246	-8%
	AMJ AMP (Max-Min)	12,745	11,802	-943	-7%
	JAS AMP (Max-Min)	6,893	6,694	-199	-3%

Units in KAF when not mentioned

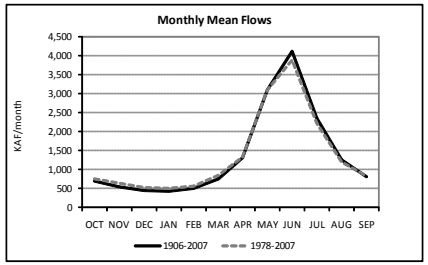

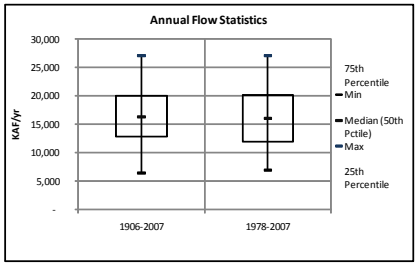

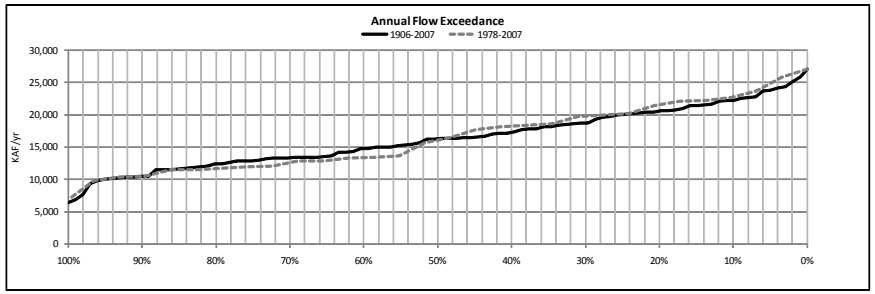

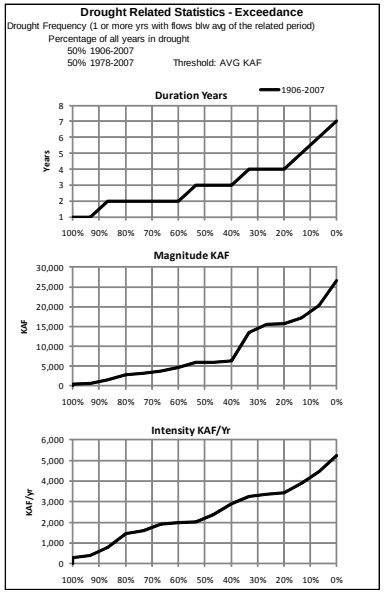

Colorado River Water Supply Analysis

Appendix B7
Watershed-based Climate and Hydrologic Process Changes

Appendix B7—Watershed-based Climate and Hydrologic Process Changes

The results of the watershed-based statistical analysis of VIC model output (climatological and hydrologic parameters) are presented for a subset of the Basin watersheds. The selected watersheds span the geographic range of the Basin. One group of watersheds was selected from the Upper Basin, and each of these watersheds contains the headwaters of a significant river. A second group of watersheds was selected from the Lower Basin, and each contains a streamflow station of significance. The selected watersheds are as follows:

Upper Basin

- 01 – Colorado River at Glenwood Springs, Colorado
- 04 – Gunnison River at Blue Mesa Reservoir
- 09 – Green River at Fontenelle
- 12 – Yampa River at Maybell
- 13 – Little Snake River at Lily
- 18 – San Juan at Archuletta
- 20 – Colorado River at Lees Ferry

Lower Basin

- 25 – Colorado River at Hoover Dam
- 29 – Colorado River Above Imperial Dam

Figures B7-1 through B7-9 depict the relative changes in monthly precipitation, temperature, evapotranspiration (ET), runoff, snow water equivalent, and soil moisture for these selected watersheds. Separate lines depict the changes for the periods 2011-2040 (2025), 2041-2070 (2055), and 2066-2094 (2080) as compared to the base period 1971-2000 (1985). The selection of time periods is explained in Appendix B-5 Section 3.3.1.

Figures B7-10 through B7-20 are spatial plots of the changes in these parameters for four seasons. The seasons are defined as: Fall (OND); Winter (JFM); Spring (AMJ); and Summer (JAS). Separate figures have been provided for the three future periods.

FIGURE B7-1
Projected Change in Mean Monthly Climatological and Hydrologic Parameters
01-Colorado River at Glenwood Springs, CO

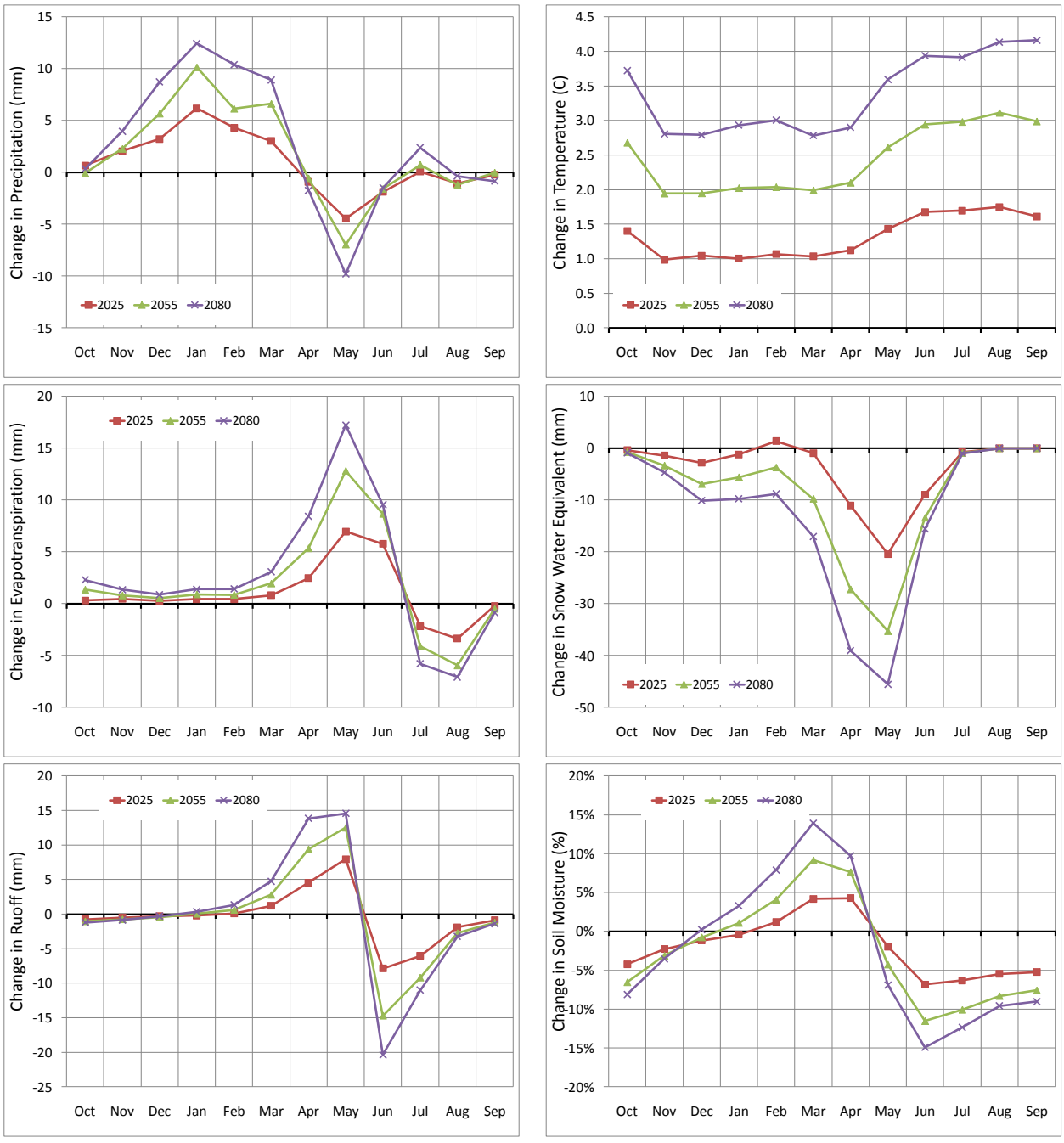

FIGURE B7-2
Projected Change in Mean Monthly Climatological and Hydrologic Parameters
04-Gunnison River at Blue Mesa Reservoir

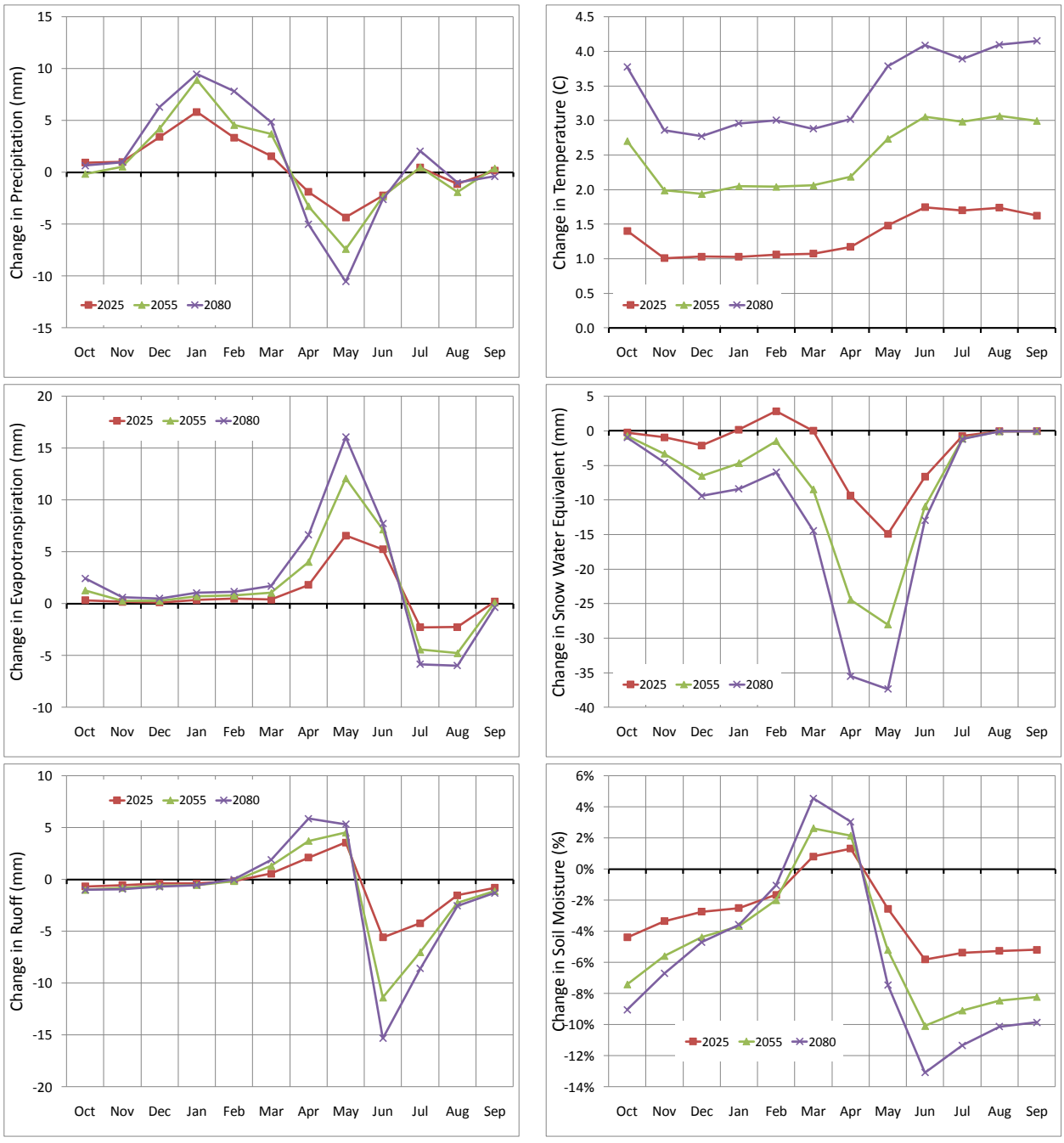

FIGURE B7-3
Projected Change in Mean Monthly Climatological and Hydrologic Parameters
09-Green River at Fontenelle

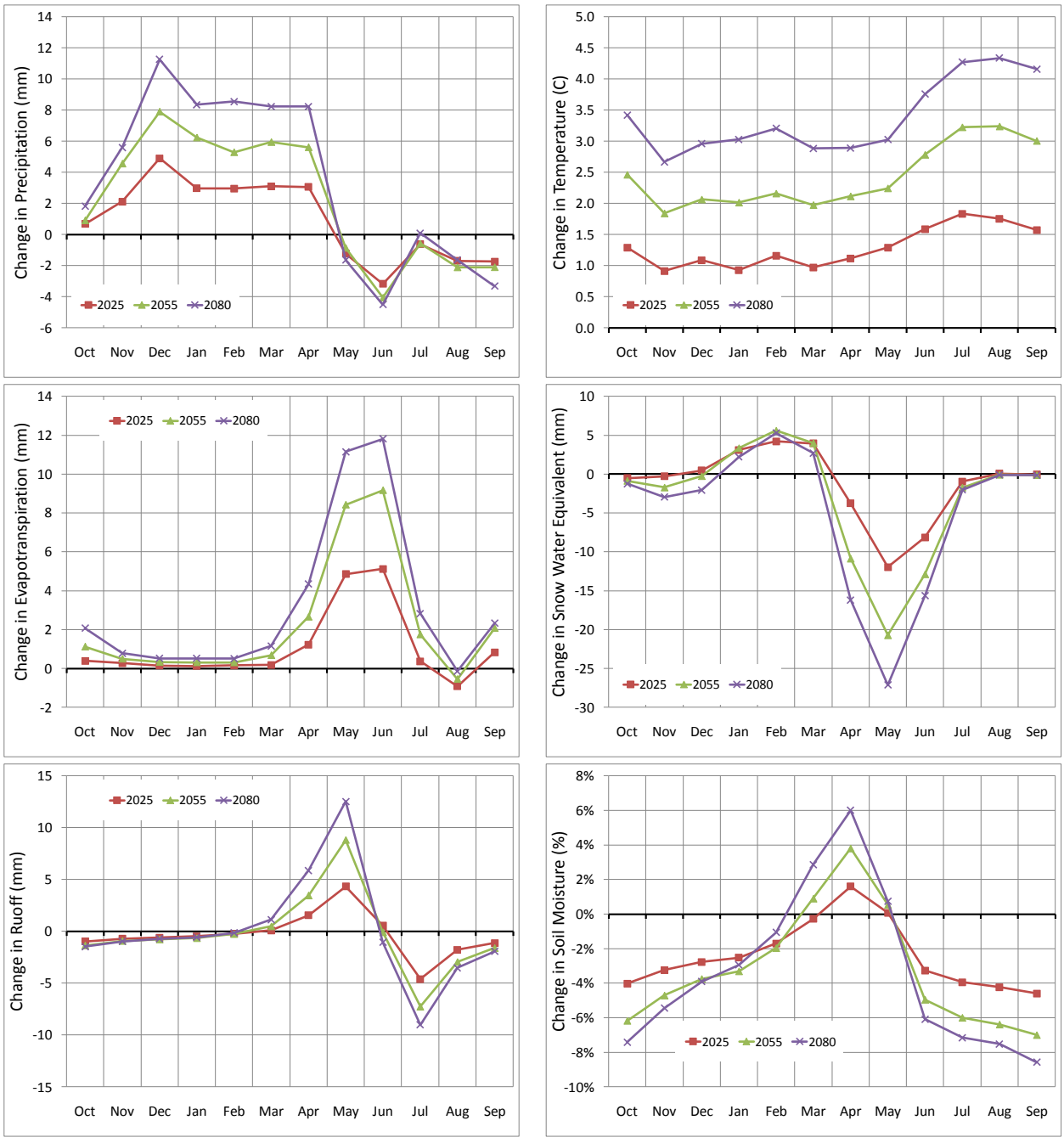

FIGURE B7-4
Projected Change in Mean Monthly Climatological and Hydrologic Parameters
12-Yampa River at Maybell

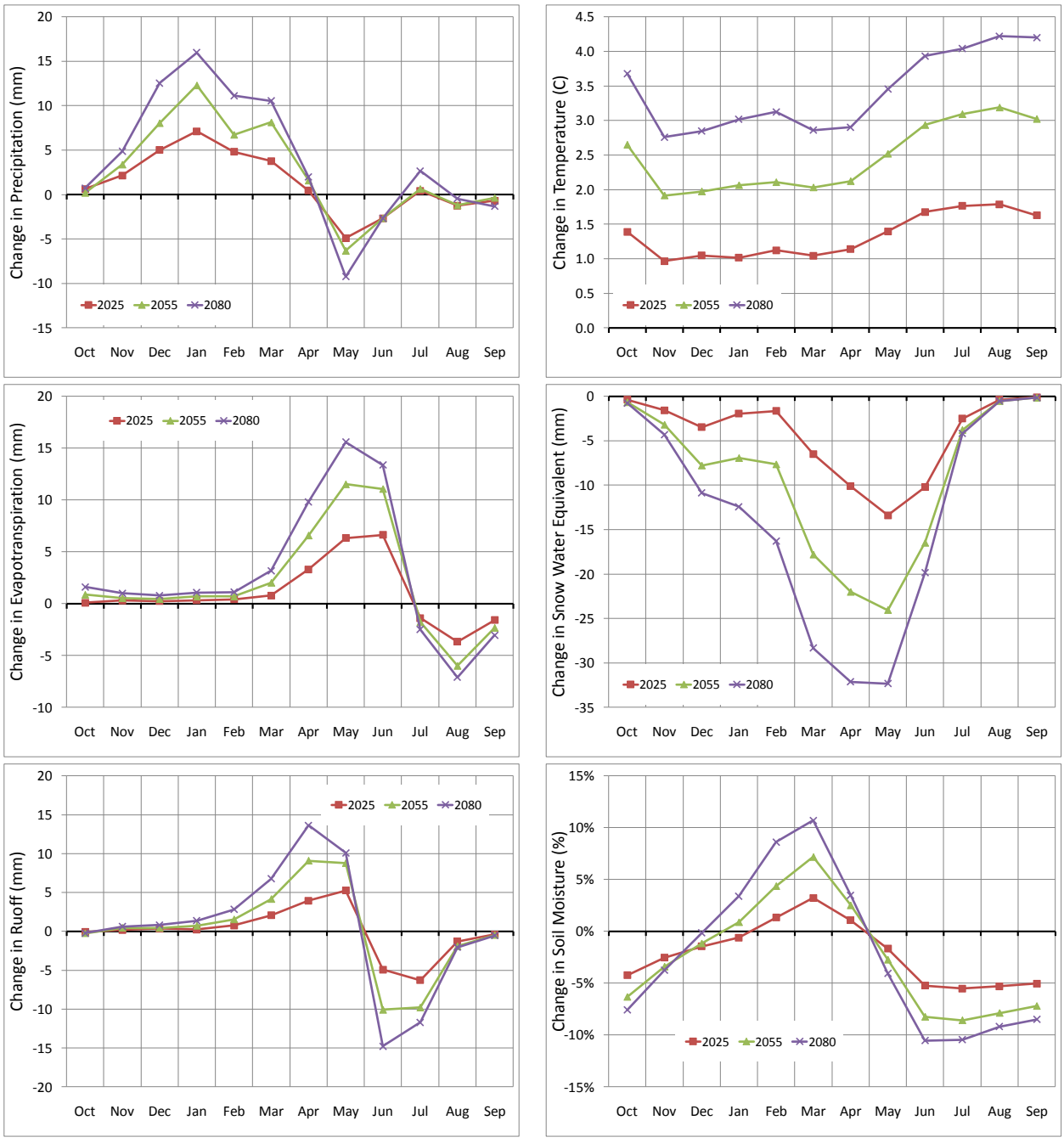

FIGURE B7-5
Projected Change in Mean Monthly Climatological and Hydrologic Parameters
13-Little Snake River at Lily

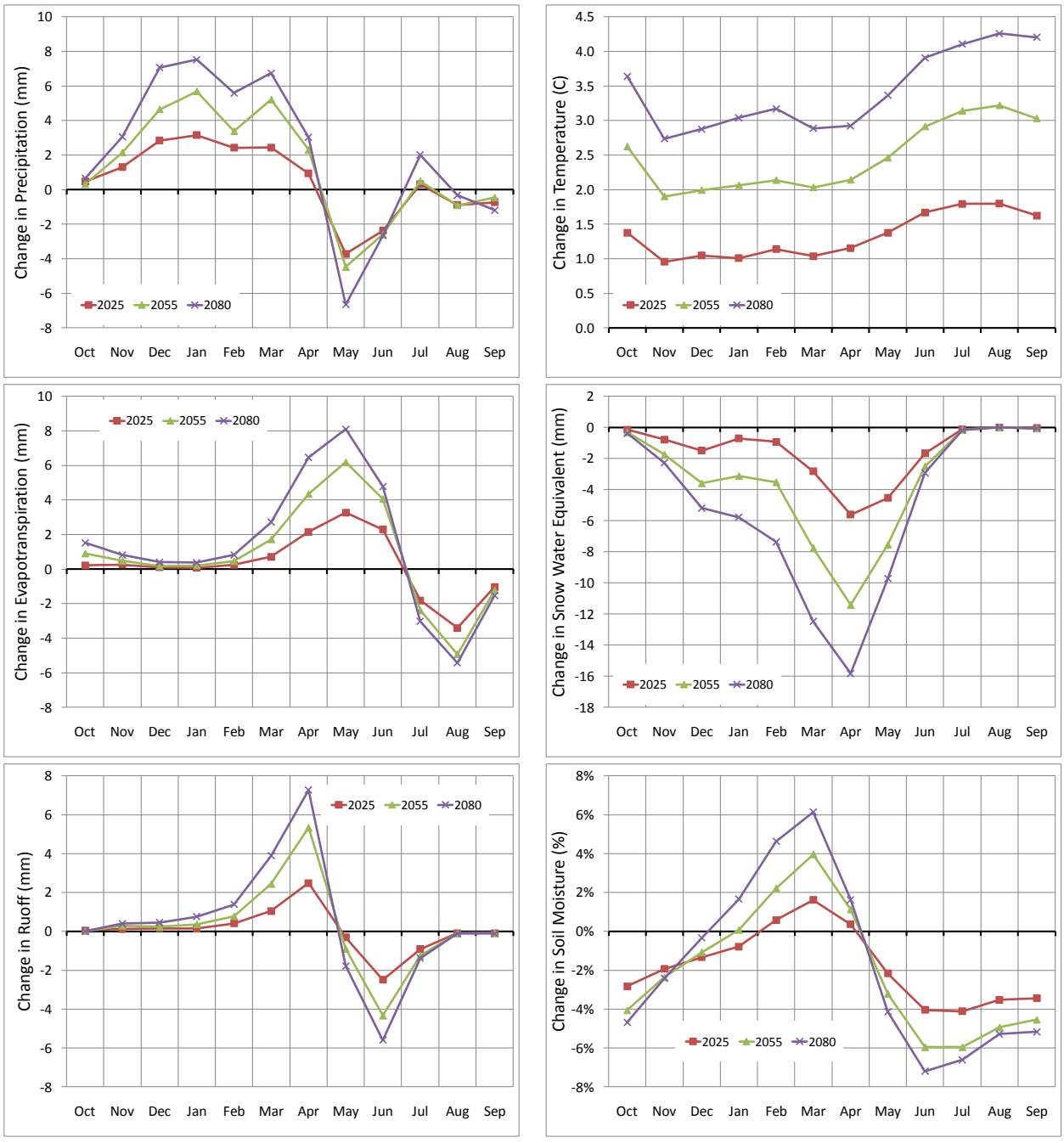

FIGURE B7-6
Projected Change in Mean Monthly Climatological and Hydrologic Parameters
18-San Juan at Archuletta

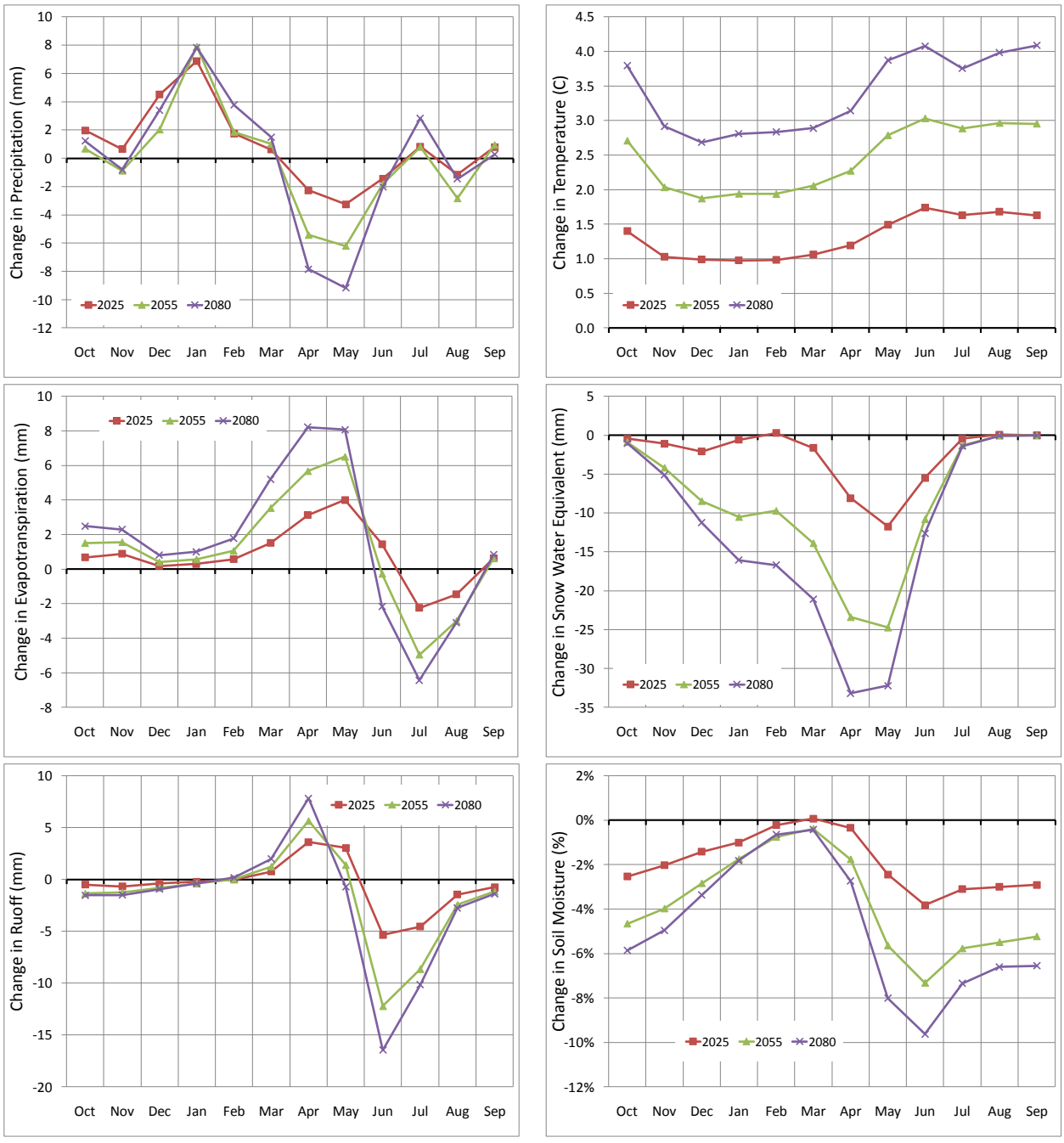

FIGURE B7-7
Projected Change in Mean Monthly Climatological and Hydrologic Parameters
20-Colorado River at Lees Ferry

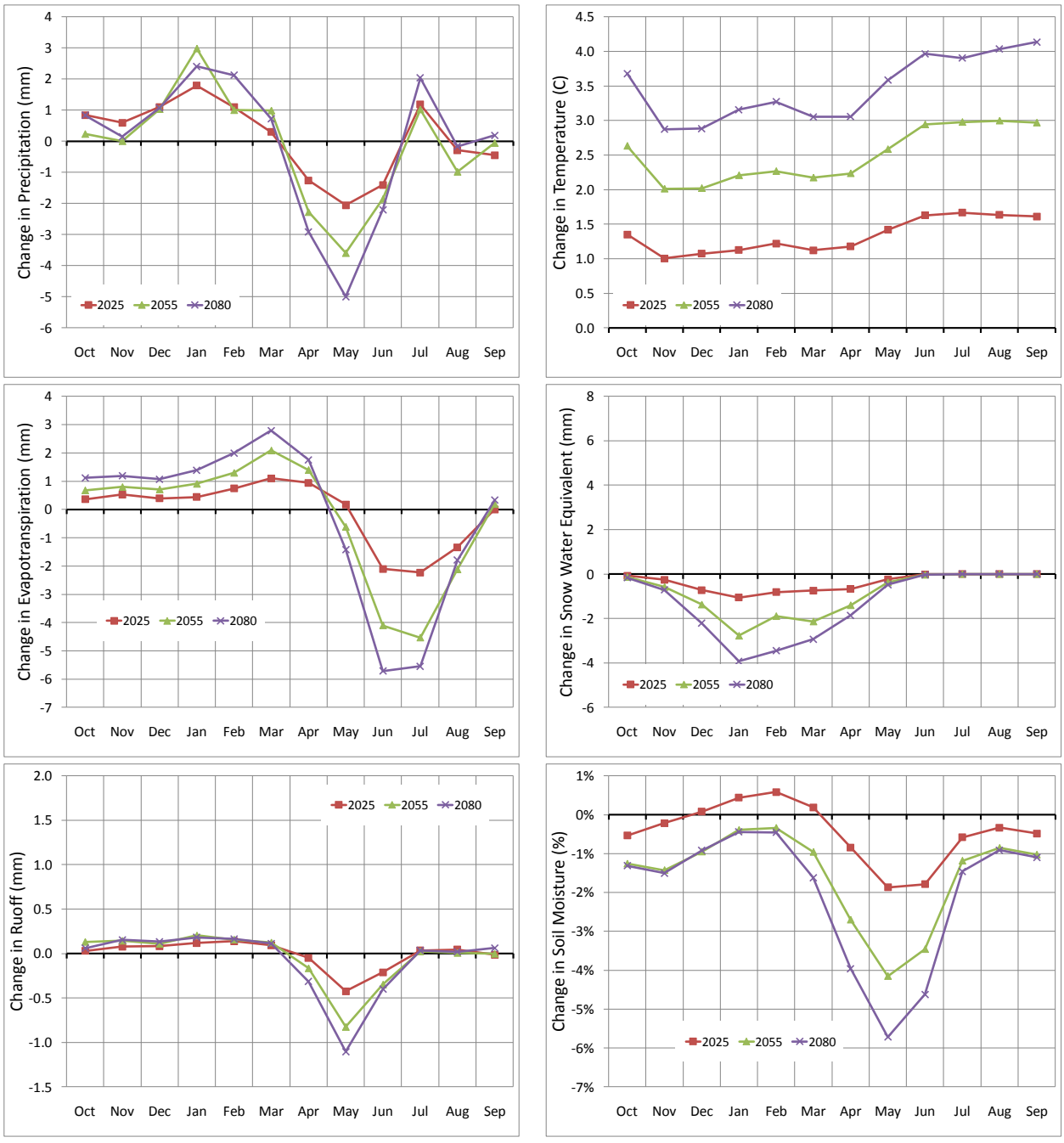

FIGURE B7-8
Projected Change in Mean Monthly Climatological and Hydrologic Parameters
25-Colorado River at Hoover Dam

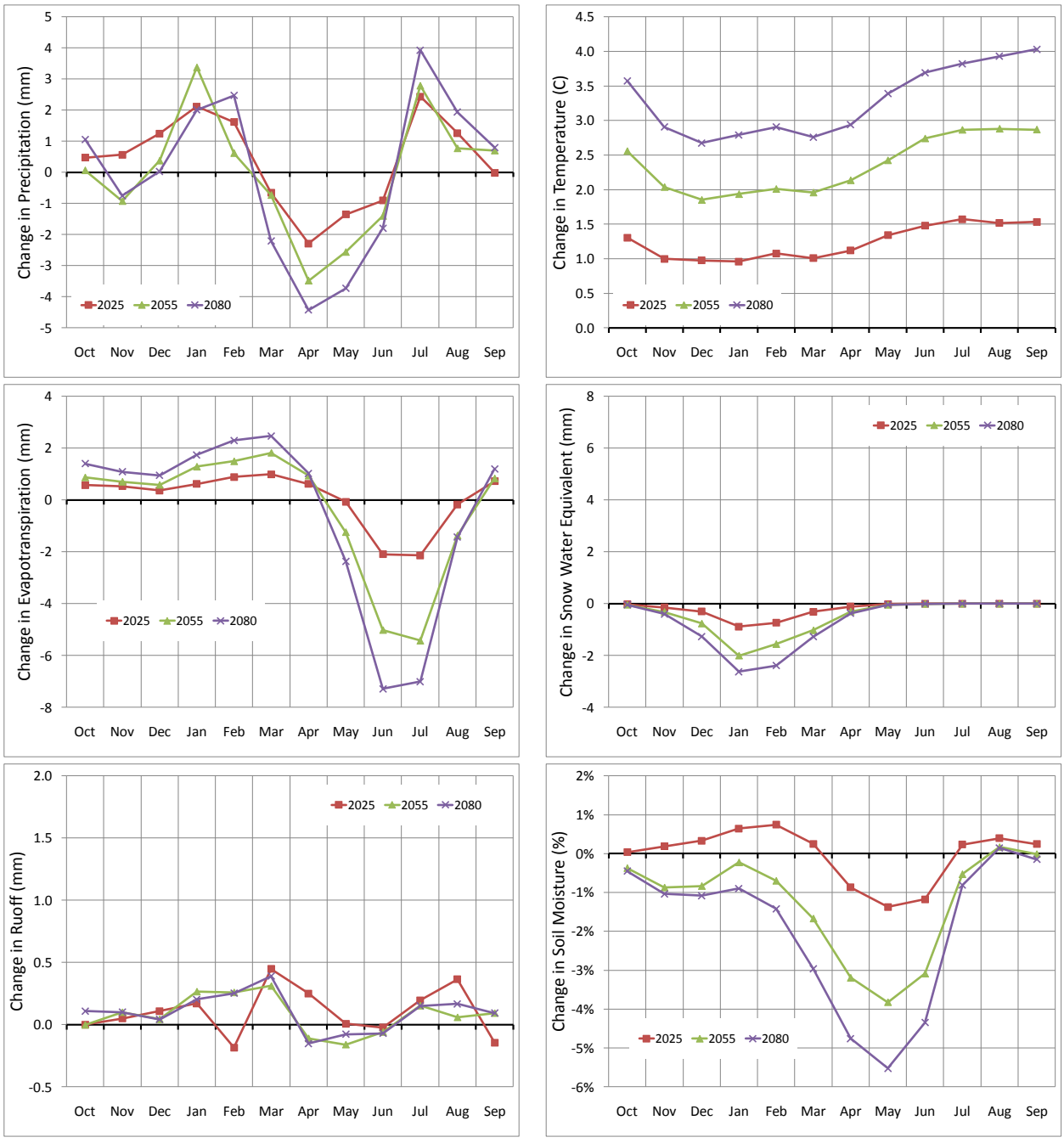

FIGURE B7-9
Projected Change in Mean Monthly Climatological and Hydrologic Parameters
29-Colorado River above Imperial Dam

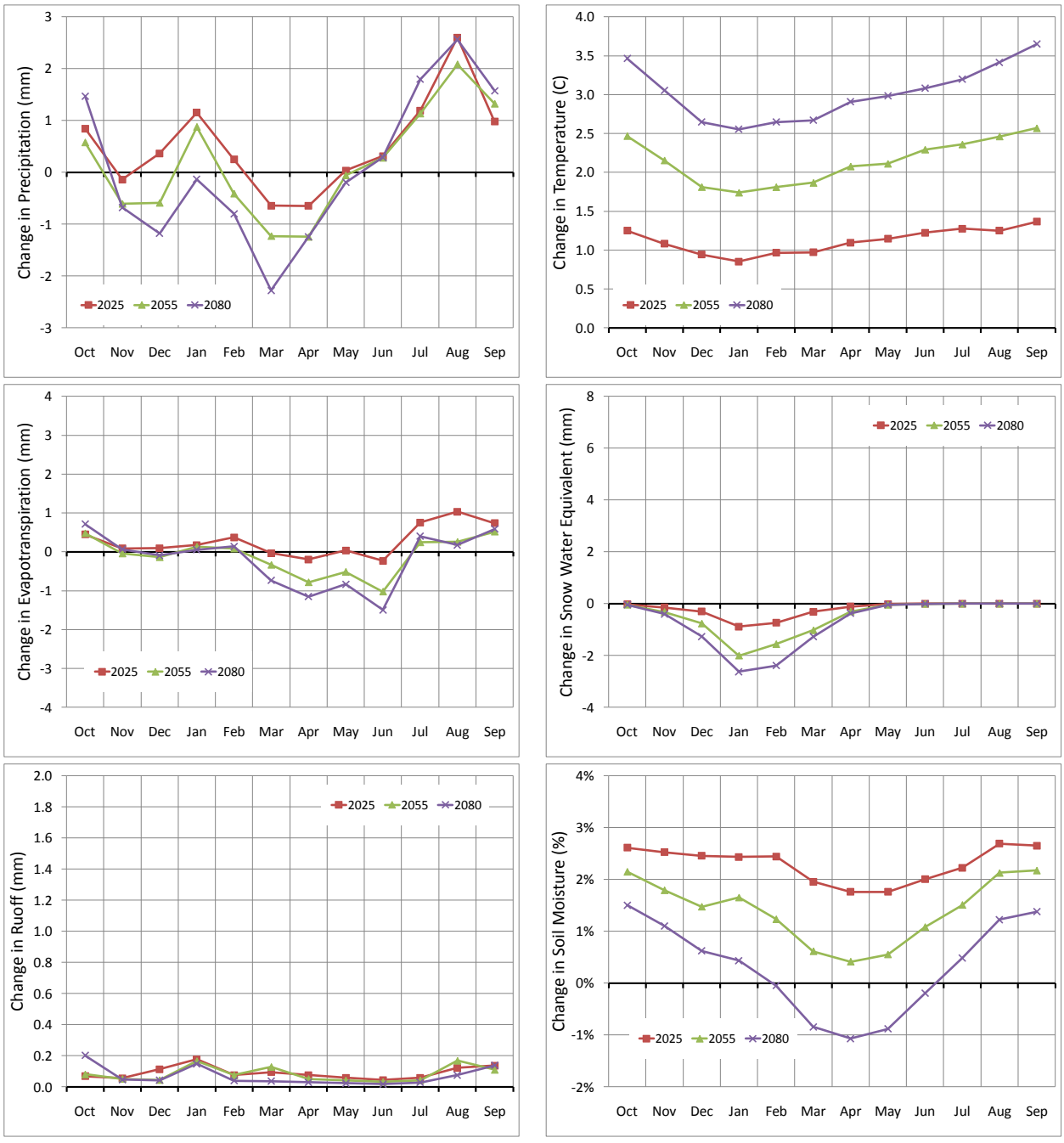

FIGURE B7-10
Projected Percent Change in Mean Seasonal Precipitation (OND is October, November, and Dec; JFM is January, February, and March; AMJ is April, May, and June; and JAS is July, August, and September)
2025 (2011 – 2040) v. 1985 (1971-2000)

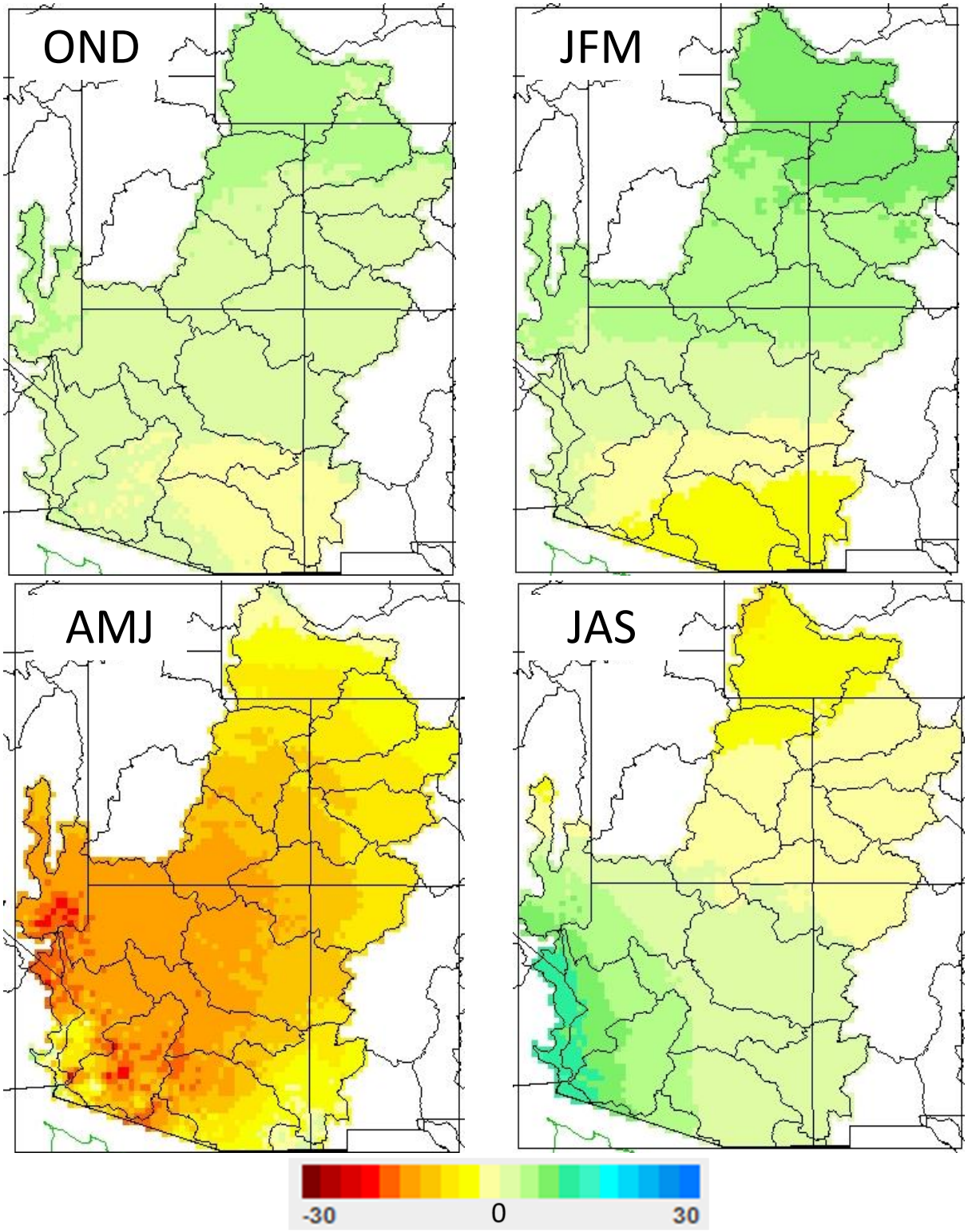

FIGURE B7-11

Projected Change (Degrees C) in Mean Seasonal Air Temperature (OND is October, November, and Dec; JFM is January, February, and March; AMJ is April, May, and June; and JAS is July, August, and September)
2025 (2011 – 2040) v. 1985 (1971-2000)

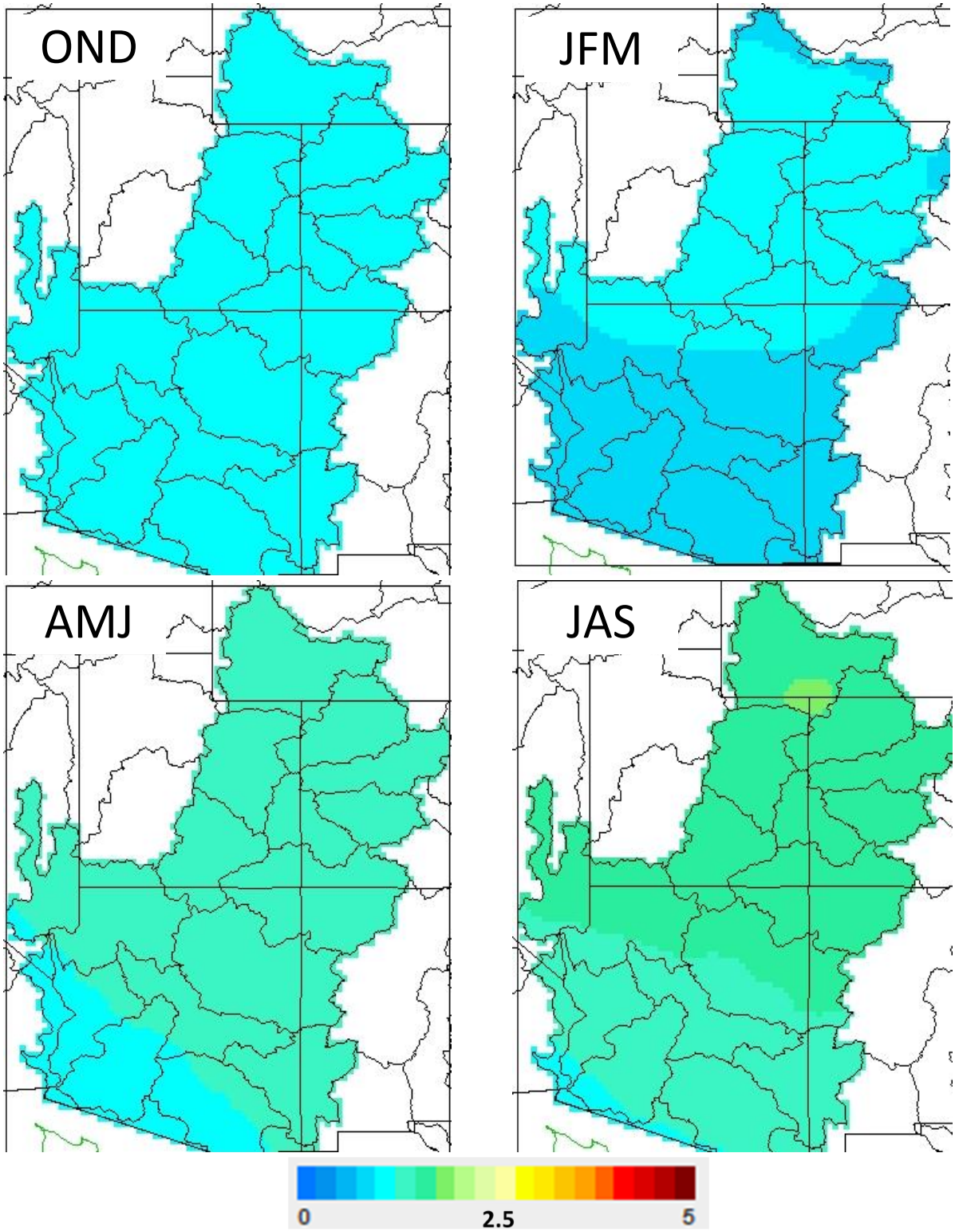

FIGURE B7-12
Projected Percent Change in Mean Seasonal Evapotranspiration (OND is October, November, and Dec; JFM is January, February, and March; AMJ is April, May, and June; and JAS is July, August, and September)
2025 (2011 – 2040) v. 1985 (1971-2000)

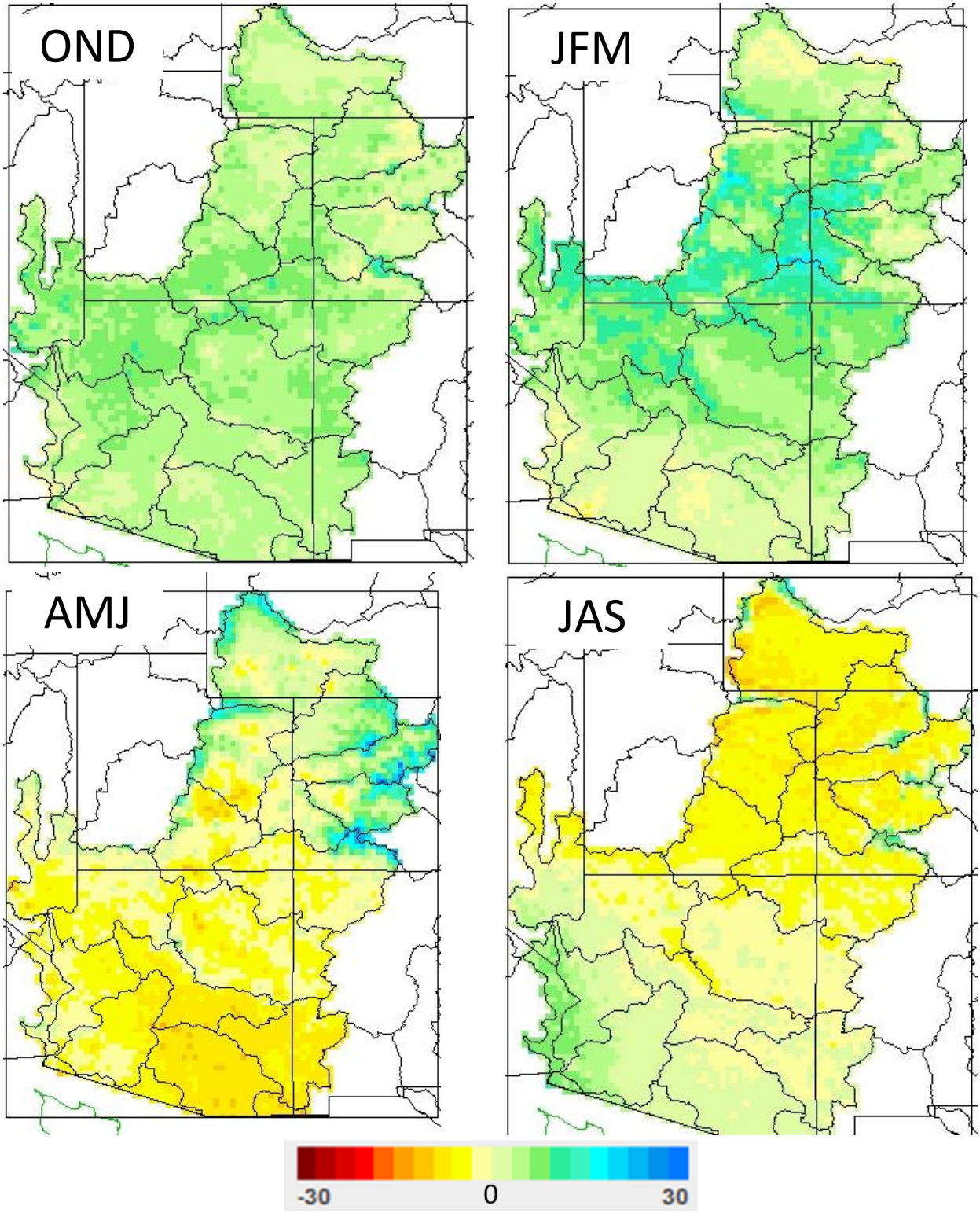

FIGURE B7-13
Projected Percent Change in Mean Seasonal Runoff (OND is October, November, and Dec; JFM is January, February, and March; AMJ is April, May, and June; and JAS is July, August, and September)
2025 (2011 – 2040) v. 1985 (1971-2000)

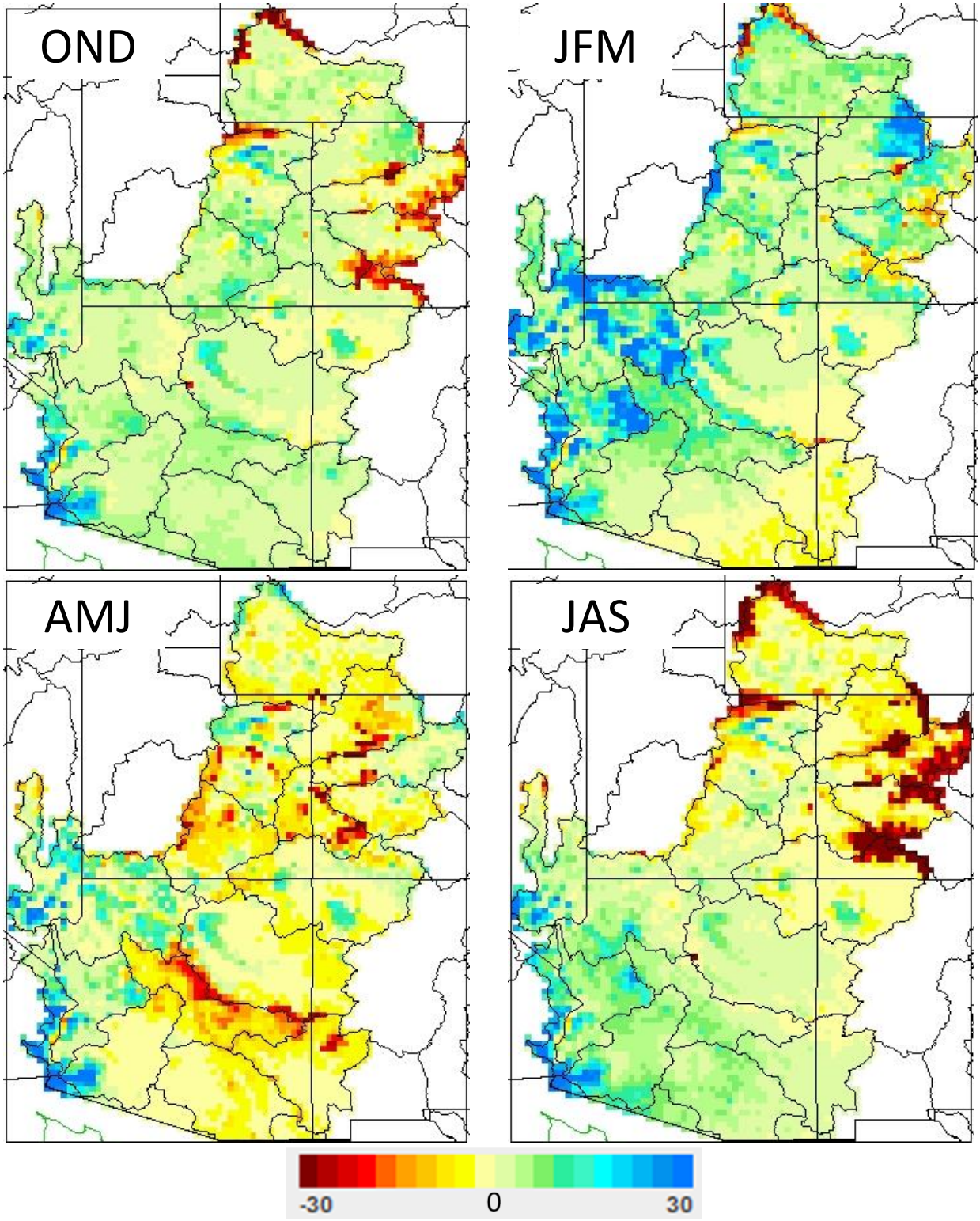

FIGURE B7-14
Projected Percent Change in Mean Seasonal Precipitation (OND is October, November, and Dec; JFM is January, February, and March; AMJ is April, May, and June; and JAS is July, August, and September)
2055 (2041 – 2070) v. 1985 (1971-2000)

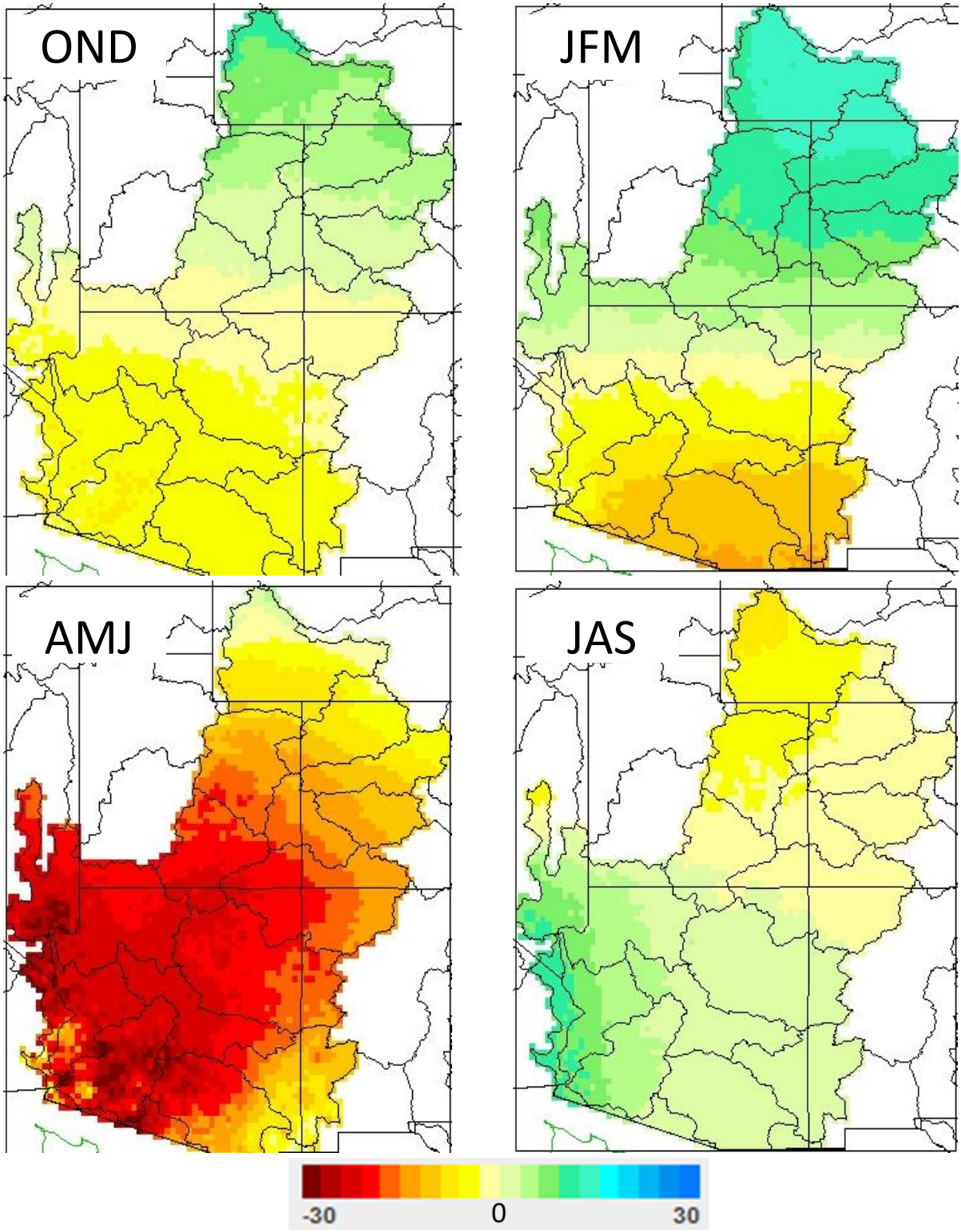

FIGURE B7-15
Projected Change (Degrees C) in Mean Seasonal Air Temperature (OND is October, November, and Dec; JFM is January, February, and March; AMJ is April, May, and June; and JAS is July, August, and September)
2055 (2041 – 2070) v. 1985 (1971-2000)

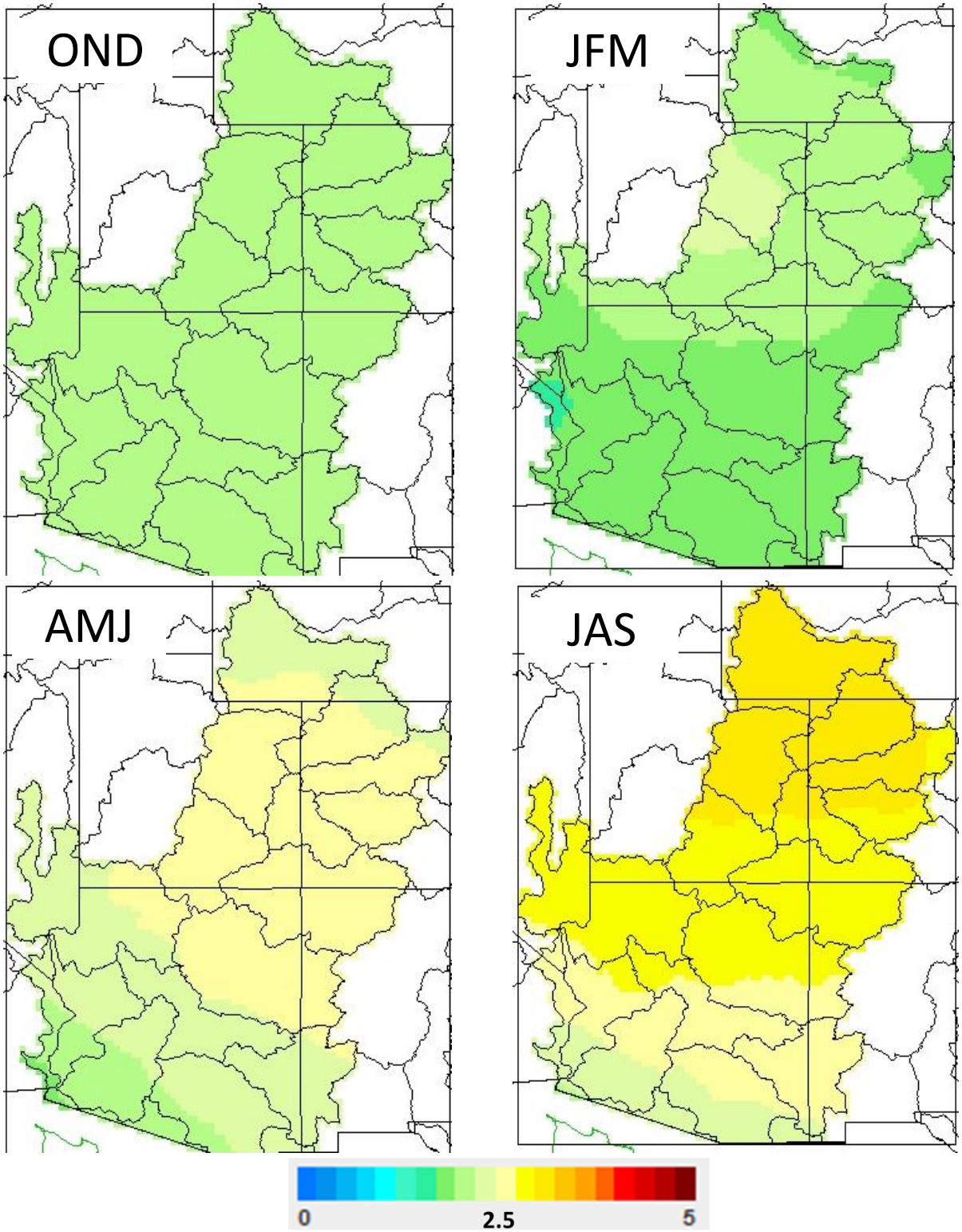

FIGURE B7-16
Projected Percent Change in Mean Seasonal Evapotranspiration (OND is October, November, and Dec; JFM is January, February, and March; AMJ is April, May, and June; and JAS is July, August, and September)
2055 (2041 – 2070) v. 1985 (1971-2000)

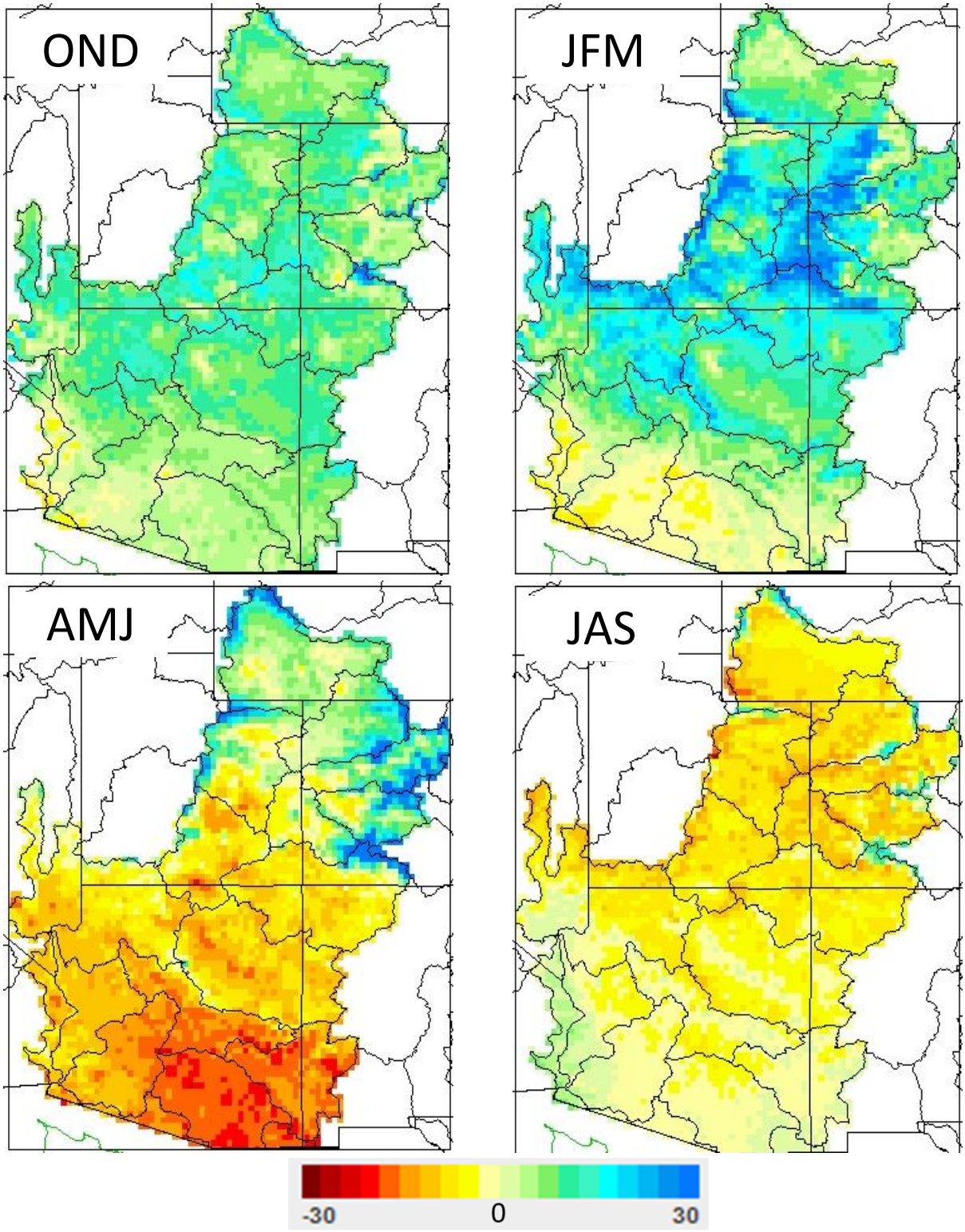

FIGURE B7-17
Projected Percent Change in Mean Seasonal Runoff (OND is October, November, and Dec; JFM is January, February, and March; AMJ is April, May, and June; and JAS is July, August, and September)
2055 (2041 – 2070) v. 1985 (1971-2000)

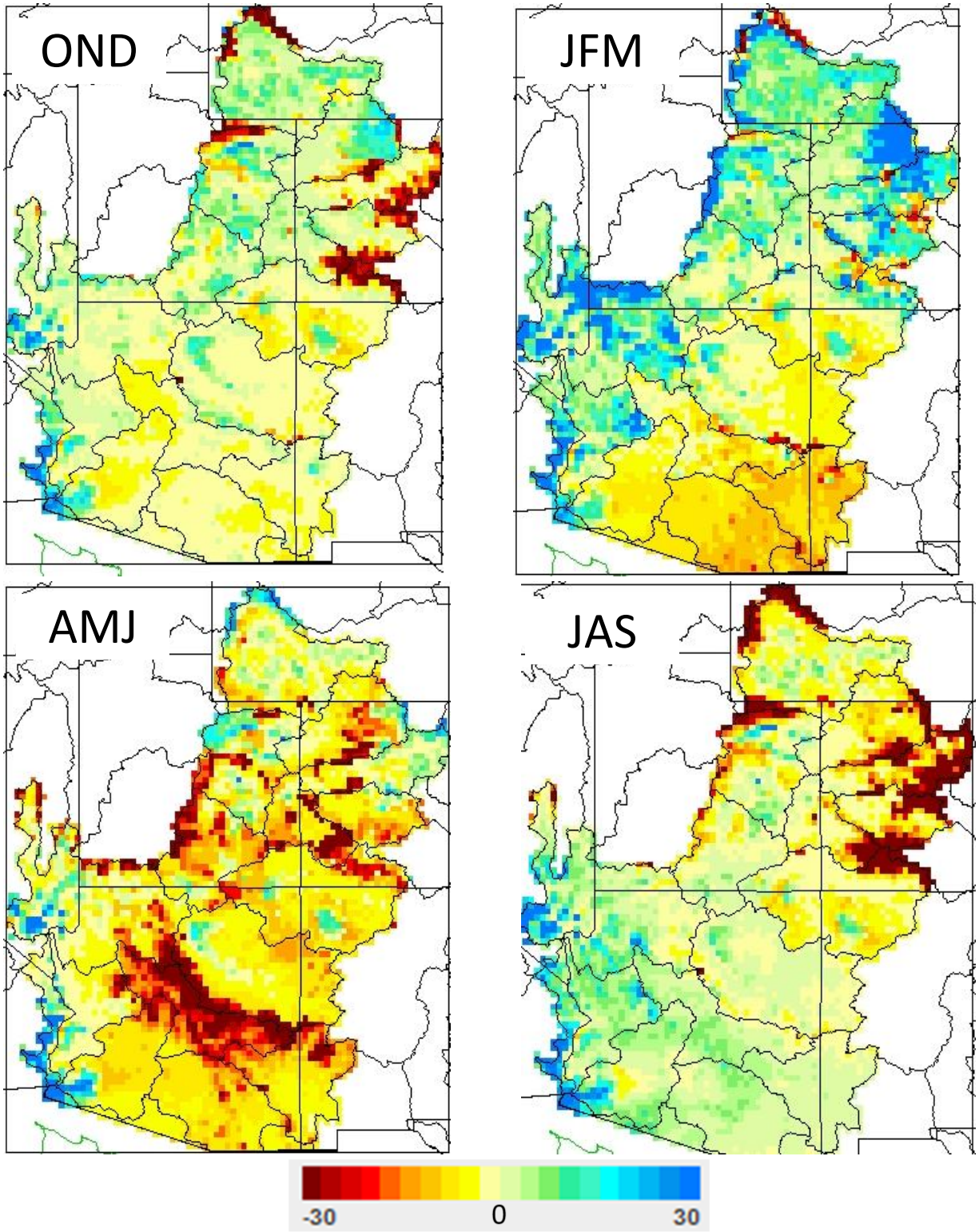

FIGURE B7-18
Projected Percent Change in Mean Seasonal Precipitation (OND is October, November, and Dec; JFM is January, February, and March; AMJ is April, May, and June; and JAS is July, August, and September)
2080 (2066 – 2095) v. 1985 (1971-2000)

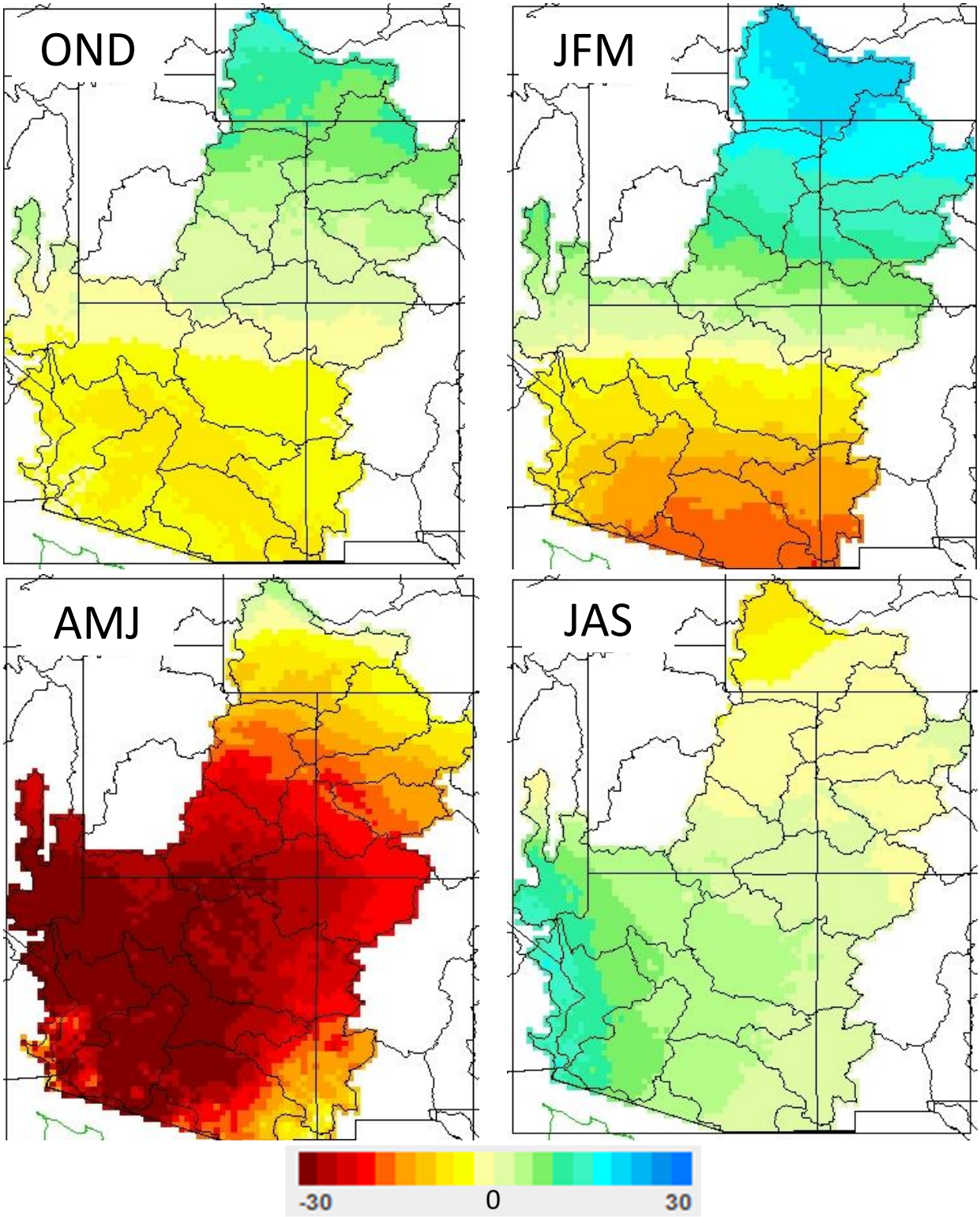

FIGURE B7-19
Projected Change (Degrees C) in Mean Seasonal Air Temperature (OND is October, November, and Dec; JFM is January, February, and March; AMJ is April, May, and June; and JAS is July, August, and September)
2080 (2066 – 2095) v. 1985 (1971-2000)

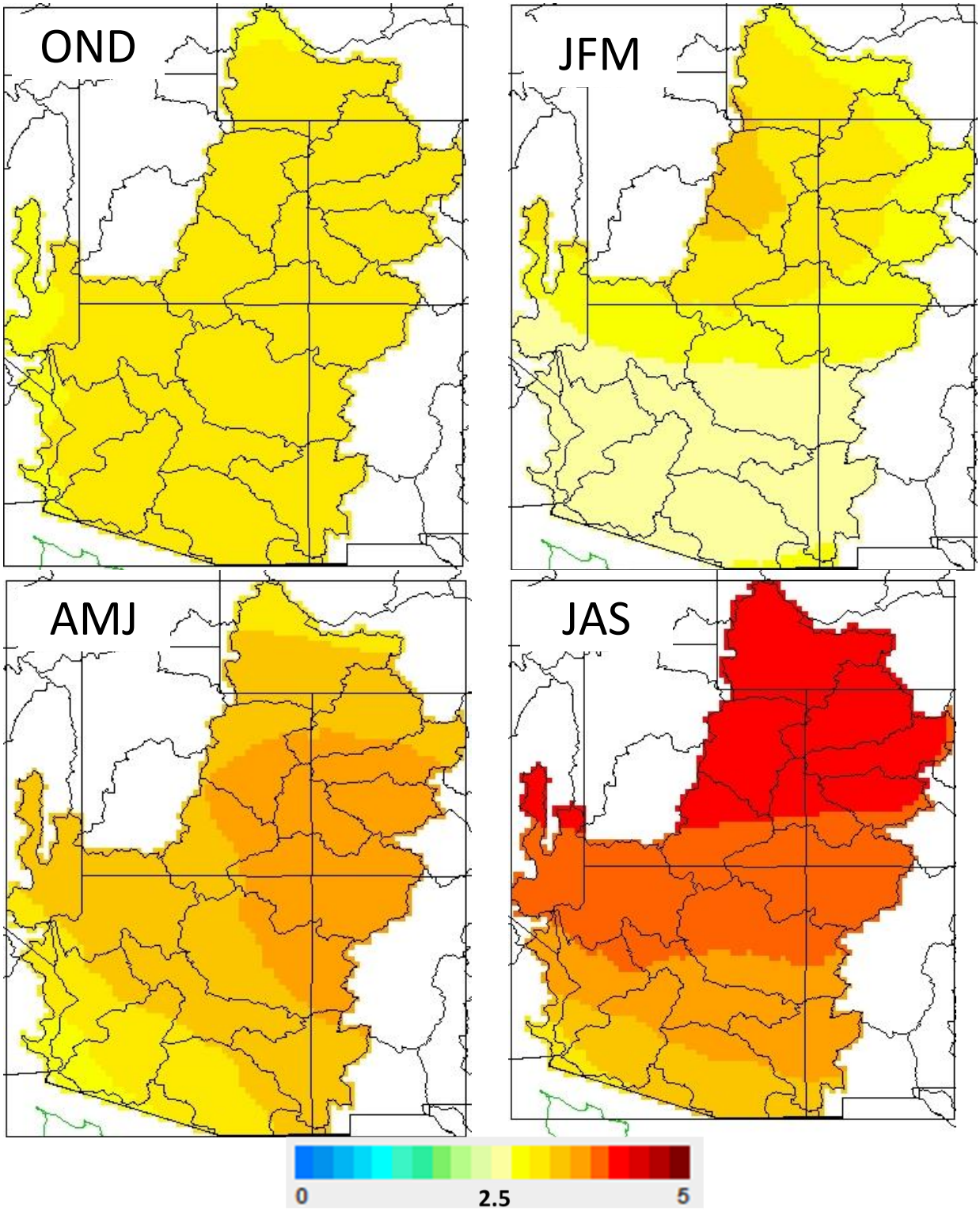

FIGURE B7-20
Projected Percent Change in Mean Seasonal Evapotranspiration (OND is October, November, and Dec; JFM is January, February, and March; AMJ is April, May, and June; and JAS is July, August, and September)
2080 (2066 – 2095) v. 1985 (1971-2000)

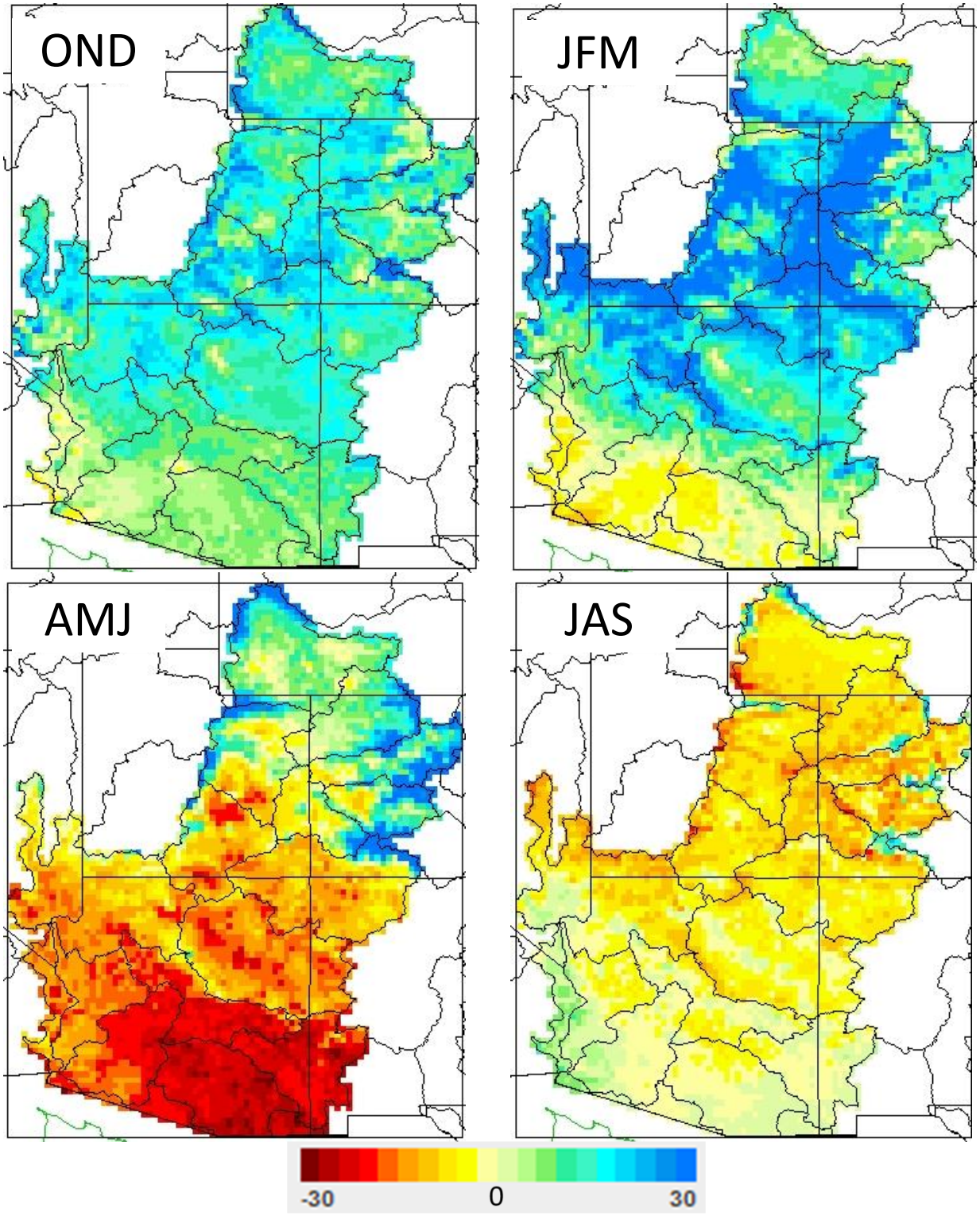

FIGURE B7-21
Projected Percent Change in Mean Seasonal Runoff (OND is October, November, and Dec; JFM is January, February, and March; AMJ is April, May, and June; and JAS is July, August, and September)
2080 (2066 – 2095) v. 1985 (1971-2000)